UNIVERSITY OF CINCINNATI

[redacted]

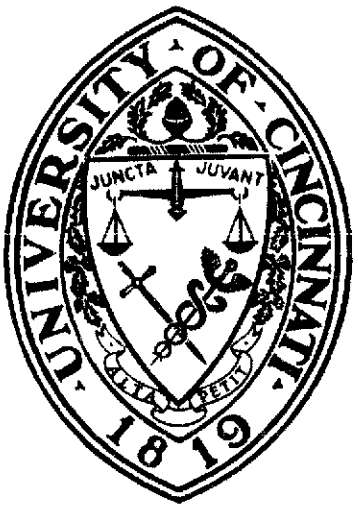

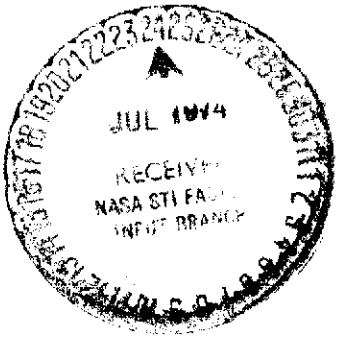

Institute of Space Sciences
University of Cincinnati
Cincinnati, Ohio 45221

Institute of Space Sciences

University of Cincinnati

Final Technical Report

for

NGR-36-004-056

Submitted to:

NASA Scientific and Technical Information Facility
P.O. Box 33
College Park, Maryland 20740

19 July 1974

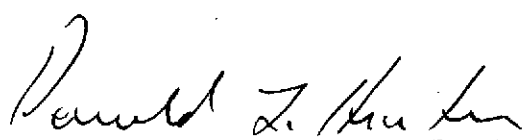

Ronald L. Huston, Director
Institute of Space Sciences

Final Technical Report

Research Grant Number: NGR-36-004-056

Origin of Grant: NASA Lewis Research Center

Name of Grantee: Institute of Space Sciences
University of Cincinnati
Cincinnati, Ohio 45221

Effective Period of Grant: 1 September 1971 - 31 May 1974

Total Amount of Grant: $ 85,059

Project Titles:

Task 1: A Study of Radiation Resistant Semiconductor Devices
Task 2: Synthesis of High Temperature Organic Lubricants
Task 3: Departure from Phase Equilibrium during Boiling Transients
Task 4: Effects of Neutron Irradiation on the Defect State in Tungsten
Task 5: Determination of Photon Response Function of NE-213 Liquid Scintillation Detectors

Principal Investigators:

Task 1: H. T. Henderson (Telephone AC 513-475-3507)
Task 2: H. Zimmer (Telephone AC 513-475-3545)
Task 3: J. Weisman (Telephone AC 513-475-2573)
Task 4: J. Moteff (Telephone AC 513-475-3096)
Task 5: A. Shapiro (Telephone AC 513-475-6393)

TASK I

A STUDY OF RADIATION RESISTANT SEMICONDUCTOR DEVICES

Principal Investigator: H. T. Henderson, Professor of Electrical Engineering

I. Introduction

This project began exclusively with work on single and double-injection devices constructed of neutron-irradiated silicon. Since the electronic properties were due to deep traps induced by very high levels of neutron radiation damage, the electrical characteristics were logically anticipated to be insensitive to a lesser radiation environment.

More recent work has concentrated on specific controllable deep-impurities in unirradiated silicon and germanium, utilized to obtain "S" type switching behavior (through double injection) and "Zener like" traps-filled-limit (TFL) behavior in single carrier injection.

It was believed that the latter devices should also be quite radiation-resistant. However the unique electrical characteristics of these devices are of independent interest. In view the diminished interest of NASA Lewis in radiation resistance, with the closing of Nuclear Systems Division, the above fact is quite relevent to the present project. The Spacecraft Technology Division of NASA Lewis is continuing the project, due to potential applications in their area of responsibility.

II. Summary of Recent Accomplishments

A. Thallium-Doped Silicon

Thallium remained as the only classical Group III acceptor basically uncharacterized in silicon. Preliminary information suggested that it should lie somewhere between 0.1 and 0.26 eV above the valence band. If the latter range were the case, calculations suggested that it could make possible an excellent double-injection switching device near room temperature.

After two years of largely futile efforts to grow thallium-doped silicon by a variety of techniques, we were able to achieve a sufficient quantity of thallium-doping to make a very accurate optical measurement of the energy level of thallium at 0.255 eV above the valence band. This is very exciting news, and we plan to report the results soon in The Physical Review.

Further, we have observed the anticipated switching behavior at room temperature, however the results are yet preliminary. The above work on thallium-doped-silicon has also resulted in the completion of a Ph.D. dissertation.

B. Trap-Filling Behavior in Pyrolytically Deposited Polycrystalline Films

An attempt was made to locate deep traps in the grain boundaries and other disordered regions of low-temperture silane-grown silicon films (amorphous-polycrystalline). The results have been positive, and the temperature-dependent characteristics conform precisely to the anticipated TFL-like behavior expected for a continuous exponential trap distribution!

Devices based upon this material should not only be radiation resistant, but they should also be very easy and inexpensive to prepare. The resulting characteristics are also Zener-like, with the slope of the vertical region of the volt-ampere curve predictably increasing with temperature.

This project will result in a completed Ph.D. dissertation within approximately one month, followed by a publication in the literature.

A further objective of the above study was the consideration of various geometries which might render these devices compatable with the planar configuration common to integrated circuit work.

C. Compensated Gold-Doped Germanium

We earlier reported the "S" type of switching behavior in gold-doped germanium (partially compensated with a shallow donor), as well as low frequency (10's of KH_z) DC-controlled bulk ocillations.

In addition to switching applications, such devices have potential application as simple and inexpensive oscillators with both amplitude and frequency-modulation capability.

Many such devices have been prepared from a variety of crystals and studied in a variety of environments. The characteristics can be controlled through a combination of temperature and magnetic field, for example. Extensive computer modeling has been applied during the past year in order to identify the details of the oscillation mechanism. The latter study has narrowed the mechanism to one of two possibilities, neither of which is the classical Gunn effect.

In this project we are also characterizing the dynamic switching behavior. Similar to amorphous switches, we have found a characteristic delay or dwell time ranging to around 10 microseconds, which can be shortened variably to zero by increasing the drive voltage. The actual switching time is around 10-30 nanoseconds.

This task will also be the subject of a Ph.D. dissertation to be completed within one or two months.

D. Optical Measurements

Since excess majority surface and bulk lifetimes (and to some extent, the minority carrier lifetimes) are important parameters in these devices, considerable attention has been given to measurement instrumentation for these quantities.

Also, the optical sensitivity of the switching behavior of the devices has potential practical applications.

Much remains to be done on the devices, but out of the instrumentation studies have unexpectedly come (1) a method for vastly increasing the sensitivity of the Haynes-Shockley method and (2) of measuring the true injection width of a p-n junction. This work is documented in a recent M.S. thesis just concluded.

III. Project Papers and Documents (Prepared Last Six Months):

(1) J.H. Nevin, Analytical and Experimental Contributions to the Characterization of Deep Impurities in IV-IV Semiconductors, Ph.D. Thesis.

(2) O.P. Saraf, Transport Studies in Germanium through Carrier Enhancement, Using Laser and Contact Injection in the Haynes-Shockley Experiment, M.S. Thesis.

(3) J.H. Nevin and H.T. Henderson, "Infrared Absorption in Thallium-Doped Silicon", to be submitted to Phys. Rev. B.

(4) J.H. Nevin, H.T. Henderson and M.K.L. Shen, "Factors Affecting the Accuracy of Energy Level Determinations in Semiconductors", to be submitted to J. Appl. Phys., J. Electronic Mat., or IEEE Tran, on Circuits.

(5) J.E. Sergent, and H.T. Henderson, "The Threshold for Double Injection with Injection-Dependent Carrier Lifetimes in the Presence of an Electron Trap in an Arbitrary Degree of Initial Occupancy", submittal undecided.

Data Complete for Following Papers:

(1) H.T. Henderson and O.P. Saraf, "A Method for Determining Effective Injection Cross-Section of a Planar Configuration".

(2) H.T. Henderson and O.P. Saraf, "Sensitivity Enhancement in the Haynes-Shockley Experiment".

(3) H.T. Henderson and M.K.L. Shen, "Variable Switching Delay Time in Gold-Doped Germanium".

(4) A. Dixit and H.T. Henderson, "Trapping Behavior in Low Temperature Silane-Deposited Silicon Films".

(5) M.K.L. Shen and H.T. Henderson, "D.C. Controllable Bulk Oscillation in Gold-Doped Germanium".

(Copies of the above papers will be submitted when reprints are made available).

Theses on Project:

Two Ph.D. theses are nearing completion, but titles have not been chosen.

TASK II

SYNTHESIS OF HIGH TEMPERATURE ORGANIC LUBRICANTS

Principal Investigator: Hans Zimmer, Professor of Chemistry

Summary

In our efforts to develop novel lubricants on the basis of organotin and organosilicon compounds, we investigated biphenylylsilicon and biphenyllytin compounds.

A total of twenty-two novel compounds were prepared and in cooperation with the Lubrication Branch of NASA's Lewis Research Center, the lubrication properties and the thermostability of these compounds were evaluated. Most of these compounds showed properties which could make them potentially useful as lubricants. Their thermostability, though fairly high in comparison with conventional lubricants, was not high enough so as to make them useful for immediate application. The results of this research were published and a reprint is reproduced as a part of this final report.

Currently, we are working on the investigation of the analogously substituted diphenylethers. Thus for, not enough compounds have been made to permit definitive conclusions to be made. We are also engaged in a small exploratory program to synthesize organotin containing polymers. Again no test results as to their usefulness have been obtained as of this date. This work is continuing with other support provided by the NASA Lewis Research Center.

Journal of Organometallic Chemistry, 63 (1973) 133–138

STERICALLY HINDERED GROUP IVB ORGANOMETALLICS

X*. PREPARATION AND SOME PROPERTIES OF BIPHENYLYLSILICON AND -TIN COMPOUNDS

HANS ZIMMER** and MARIA ANGELES BARCELON
Department of Chemistry, University of Cincinnati, Cincinnati, Ohio 45221 (*U.S.A.*)
WILLIAM R. JONES Jr.
NASA, Lewis Research Center, Lubrication Branch, Cleveland, Ohio 44135 (*U.S.A.*)
(Received March 30th, 1973)

SUMMARY

A representative number of *meta*- and *para*-trialkylsilicon and trialkyltin substituted biphenyls have been synthesized and their thermostability determined. The silicon compounds were found to be more heat resistant than the corresponding tin compounds. No significant difference in the thermostability between the *meta*- and *para*-substituted compounds seems to exist.

Our investigations of the preparation and some of the chemical and physical properties of sterically hindered Group IVB organometallic compounds have been extended to include the biphenylyl group. One of the goals of the present study was to synthesize resistant high-temperature organosilicon and organotin compounds, and test their suitability as lubricants. Besides thermal stability, therefore, these compounds had to be liquids over an extended temperature range. It was thought that compounds of the general structure

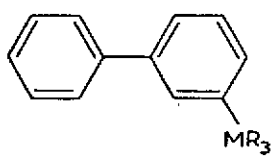

would come close to possessing the desired properties. Staab[2] found the *meta*-linked oligophenylenes to exhibit remarkable thermal stability. The investigation of the *meta*-biphenylyl derivatives was therefore chosen in preference to the *para*-biphenylyl derivatives. A representative number of *para*-substituted biphenyls were also synthesized and included in this study. Though a few biphenylyltin and silicon

* For part IX see ref. 1.
** To whom inquiries should be adressed.

compounds have been prepared[3-5], no systematic investigation of the biphenylyl group as substituent in silicon and tin organics has been made.

RESULTS

Synthesis

The compounds used in this study were prepared by allowing the magnesium or lithium derivative of *m*- or *p*-bromobiphenyl to react with the appropriate triorganotin or triorganosilicon chloride. Attempts to substitute the bromobiphenyl with the corresponding chlorobiphenyl were unsuccessful. The synthesis of the desired compounds posed similar problems as have been reported by earlier investigators[6]. For no apparent reason certain compounds could only be obtained via the corresponding lithium reagents, while with others, the desired product could be prepared only if the appropriate Grignard compound was employed. Generally, once the metal (Li or Mg) was chosen, the *meta* derivatives could be prepared and purified with less difficulty than the *para* derivatives; this is true for the tin as well as the silicon series. The work-up and preparation of pure material was often rather tedious due to the presence of by-products, such as biphenyl, various coupling products, and in the case of the tin organics, the hexaalkylditins. Most of the compounds could be obtained in a pure state only by repeated vacuum distillation. The fractions were monitored by VPC and NMR-spectroscopic methods. Only cuts which showed chemical shifts in the aromatic as well as aliphatic region were collected and further purified. Attempts to obtain the desired compounds by treating the *m*- or *p*-biphenylyltin trichloride with the appropriate alkyllithium compounds were abandoned when it was found that the preparation and purification of biphenylyltin trichloride according to a Kocheshkov reaction led to a mixture of tetrabiphenylyltin, mono-, di-, and trichlorides, which was exceedingly difficult to separate.

Thermostability

As an indication for the thermal stability of the biphenylyltrialkylsilicon and tin compounds, their decomposition temperature (T_D) was measured[7]. A common method of determining the thermal stability of organic compounds is by measuring time rate of vapor pressure rise with increasing temperature. The T_D is determined from a plot of the logarithm of the vapor pressure as a function of the reciprocal of absolute temperature. The temperature at which the vapor pressure curve deviates from linearity is taken as the decomposition temperature. The T_D may also be determined from isothermal rates of pressure rise. Several rates are measured and the logarithm of rate of pressure rise is plotted as a function of the reciprocal of absolute temperature. The decomposition temperature is taken to be that temperature at which the rate of pressure rise is 50 mm per hour[8]. This latter procedure was used to determine T_D of the compounds prepared in this study (Tables 1 and 2).

Inspection of the data reveals that in every case the silicon compounds are thermally more stable than the corresponding tin compounds. Generally, there is a difference in T_D's of 40–50° in favor of the silicon compounds. In the tin series, there seems to be no difference in the thermal stability between the *meta*- and *para*-biphenylyl derivatives. A possible explanation of this behavior might be that the thermostability of the compounds is determined by the Sn–C bond strength of the tin–carbon bond

TABLE 1

BIPHENYLYL-SUBSTITUTED TIN COMPOUNDS

Compounds[a]	*Method of synthesis*	T_D	*Yield* (%)	*B.p*(°C/*mm*) *or m.p*(°C)	*Analysis*[b]*, found (calcd.)* (%)	
					C	*H*
m-BphSnMe$_3$	B	230	87	105/0.005	56.65 (56.83)	5.73 (5.73)
p-BphSnMe$_3$[c]	B		40	50	57.02 (56.83)	5.84 (5.73)
m-BphSnPr$_3$	B	236	46	145–55/0.06	62.23 (62.87)	7.7 (7.53)
p-BphSnPr$_3$	B	240	60	155–65/0.01	62.66 (62.87)	7.25 (7.53)
m-BphSnBu$_3$	B	236	75	159–62/0.03	64.78 (65.03)	7.95 (8.18)
p-BphSnBu$_3$	B	240	46	175–85/0.01	65.29 (65.03)	8.40 (8.18)
m-BphSn(CH$_2$CMe$_3$)$_3$	AB	283	72	88.5–89	66.6 (66.81)	8.77 (8.72)
m-BphSn(n-C$_6$H$_{13}$)$_3$	AB	236	26	180–95/0.005	68.34 (68.31)	9.24 (9.17)
m-BphSn(n-C$_7$H$_{15}$)$_3$	AB	260	53	214–20/0.02	69.75 (69.59)	9.35 (9.55)
m-BphSn(CH$_2$CHEtBu)$_3$	AB	260	30	200–09/0.01	71.3 (70.7)	9.92 (9.88)
m-BphSn(n-C$_8$H$_{17}$)$_3$	AB		34	238–46/0.03	70.71 (70.7)	10.06 (9.88)
p-BphSnPh$_3$	B	297	33	120–23	71.37 (71.6)	4.82 (4.81)
(*m*-Pr$_3$SnC$_6$H$_4$)$_2$	B	214	42	130/0.06	55.57 (55.59)	7.74 (7.77)

[a] Bph = $C_6H_5C_6H_4$. [b] NMR spectra of all compounds were taken to corroborate the elemental analyses. [c] Previously reported in ref. 5.

between the biphenylyl group and the trialkyltin moiety, and differences in the stability of the resulting biphenylyl radicals are not determining factors. Though only a few examples are available for comparison in the silicon series, a similar trend seems to exist here.

The data further reveal that all the biphenylyltrialkyltin compounds with alkyl groups of little steric requirements (methyl to n-butyl) have practically identical T_D's. It is noteworthy that the trineopentyltin homolog, in agreement with our previous findings[9], is by a considerable margin the most heat resistant among the tin compounds. The T_D of the *m,m'*-bis(tri-n-propyltin)biphenyl is rather unexpectedly low.

The T_D's of the silicon derivatives seem to increase with increasing chain length of the alkyl group, with the tri-n-octylsilicon derivative being stable to about 350°.

Since the trends in thermostability with both elements were similar, the most heat-resistant compound of this type should be *m*-(trineopentylsilyl)biphenyl. Considerable efforts were made to synthesize this compound. However, probably due to steric hindrance, we were unable to make the necessary trineopentylchloro- or

TABLE 2

BIPHENYLYL-SUBSTITUTED SILICON COMPOUNDS

Compound[a]	*Method of synthesis*	T_D	*Yield* (%)	*B.p*(°C/mm) *or m.p.*(°C)	*Analysis*[b], *found (calcd.)*(%)	
					C	*H*
m-BphSiMe$_3$[c]	B	278	76	78–82/0.03	79.42 (79.58)	8.11 (8.02)
p-BphSiMe$_3$[d]	C	311	34	45	79.39 (79.58)	7.85 (8.02)
m-BphSiEt$_3$	B	296	56	117–25/0.07	80.79 (80.52)	8.93 (9.01)
p-BphSiEt$_3$[d]	C		46	125/0.02	80.70 (80.52)	8.7 (9.01)
m-BphSiPr$_3$	C	276	75	125–31/0.02	81.20 (81.21)	9.77 (9.73)
m-BphSiBu$_3$	B	295	78	159–60/0.04	81.58 (81.74)	10.38 (10.29)
p-BphSiBu$_3$[e]	C	300	36	162–64/0.01	80.91 (81.74)	9.98 (10.29)
m-BphSi(n-C$_6$H$_{13}$)$_3$	B	300	31	185–90/0.02	82.20 (82.49)	10.84 (11.07)
m-BphSi(n-C$_8$H$_{17}$)$_3$	B	358	71	215–20/0.005	83.07 (82.99)	11.51 (11.61)

[a] Bph = $C_6H_5C_6H_4$. [b] NMR spectra of all compounds were taken to corroborate elemental analysis. [c] Ref. 4. [d] Ref. 3. [e] NMR spectrum showed the right proportion of aliphatic to aromatic protons, therefore the compound was not redistilled for further purification.

-bromosilane. There are several reports in which the failure of the synthesis of R_4Si compounds with four large and bulky groups was believed due to steric hindrance around the silicon atom[10].

EXPERIMENTAL

Synthesis

The biphenylyl–silicon and –tin compounds were prepared by the reaction of either a Grignard reagent derived from biphenyl, or of a lithiobiphenyl compound, with the trialkylhalo derivative of tin or silicon. No attempt was made to optimize the yields and all boiling points as well as melting points are uncorrected. Microanalyses were performed by Galbraith Laboratories Inc., Knoxville, Tennessee. The following detailed descriptions should serve as examples for the methods used for the preparation of the compounds.

Triheptyltin chloride (*Scheme A*) To a mixture of 75 ml of dry tetrahydrofuran (THF) and 5.86 g (0.24 g-atom) of magnesium turnings was added 10 g (0.08 mole) of heptyl chloride. The mixture was stirred and gently warmed until it was evident that the reaction had started. More THF was then added and the rest of the heptyl chloride, 22.07 g (0.16 mole) in 25 ml of THF, was added dropwise. The reaction mixture was refluxed until most of the magnesium turnings had disappeared. The heating was

then discontinued and a solution of 15.63 g (0.06 mole) of stannic chloride in benzene was added at room temperature. The reaction mixture was stirred and refluxed overnight and decomposed by adding a saturated ammonium chloride solution to the mixture. The organic layer was separated, washed, and dried over anhydrous magnesium sulfate. The oil obtained was dissolved in ether, saturated with anhydrous gaseous HCl and allowed to stand for two days. Excess acid and solvent were removed and the remaining mixture was fractionally distilled to give 22.7 g of triheptyltin chloride (83% yield). (Found: C, 56.19; H, 10.00. $C_{21}H_{45}ClSn$ calcd.: C, 55.83; H, 10.04%.

The preparation of *trineopentyltin chloride*[9] from tetraneopentyltin was accomplished by a Kocheshkov reaction in benzene by heating a mixture of 3/1 mole ratio of the tetraorganotin and stannic chloride at reflux (80°) for 48 h.

m-Biphenylyltriheptyltin (*Scheme B*). A Grignard solution was prepared from 0.97 g (0.04 g-atom) of magnesium and 9.32 g (0.04 mole) of *m*-bromobiphenyl in 150 ml of THF. To this mixture a solution of 13.55 g (0.03 mole) of triheptyltin chloride in THF was gradually added and then refluxed for 1 h. The solvent was changed to xylene and the mixture was heated at reflux overnight. After the usual work-up, the resulting heavy liquid was fractionated under reduced pressure, to give 9.7 g (53%) of *m*-biphenylyltriheptyltin boiling between 214 and 220° at 0.02 mm.

m-Biphenylyltripropylsilane (*Scheme C*). A mixture of 1.13 g (0.08 g-atom) of lithium wire, cut into small pieces, and 50 ml of anhydrous ether was stirred under argon and reacted with 18.77 g (0.08 mole) *m*-bromobiphenyl. After almost all the lithium had disappeared, 12.48 g (0.06 mole) of tripropylchlorosilane in ether was gradually added. The ether solvent was then replaced with benzene and the resulting mixture refluxed for 12 h.

The reaction mixture was hydrolyzed with dilute sulfuric acid and the organic layer was separated and dried over anhydrous magnesium sulfate. Fractional distallation gave 15 g (75%) of *m*-biphenyltripropylsilane distilling between 125 to 131° at 0.02 mm.

Thermostability

The tensimeter used for determining the T_D's in this study consists of two units: the sample oven with an associated temperature programmer and the electronics module containing the recorder. The function of a tensimeter is to heat a liquid sample and plot either the vapor pressure, or the isothermal rate of increase of vapor pressure (due to thermal decomposition), as a function of temperature.

Procedure. Three to four mls. of test fluid are placed in the sample cell. The cell is attached to the cell assembly and the fluid is degassed and refluxed under vacuum. The cell assembly is then placed in the oven. The sample is heated to an initial temperature about 50° below the suspected decomposition temperature. After a 5-minute stabilization period, the increase in vapor pressure, if any, is recorded as a vertical bar during a fixed time interval. Then the programmer raises the sample temperature by a preset amount, usually 5°, and the previous process is repeated. The plot one obtains essentially is a plot of the logarithm of the isothermal rate of vapor pressure increase as a function of reciprocal absolute temperature. A straight line is drawn connecting the tops of the recorded bars at the higher temperatures. The intersection with the temperature reference axis is the thermal decomposition

temperature, T_D. This temperature axis corresponds to a pressure rise of 50 mm per hour, which is the definition of the T_D. Generally, it is possible to dupicate the T_D's within $\pm 5^\circ$ for pure compounds.

ACKNOWLEDGEMENT

This research was generously supported by NASA-Grants, NGR 36-004-043 and NGR 36-004-056.

REFERENCES

1 H. Zimmer and A. V. Bayless, *Tetrahedron Lett.*, (1970) 459.
2 H. A. Staab and C. Wuensche, *Chem. Ber.*, 101 (1968) 887.
3 A. D. Petrov and T. I. Chernysheva, *Doklady Akad. Nauk SSSR*, 84 (1952) 515.
4 H. Gilman and G. Lichtenwalter, *J. Org. Chem.*, 21 (1956) 1307.
5 M. D. Curtis and A. L. Allred, *J. Amer. Chem. Soc.*, 87 (1965) 2554.
6 L. W. Breed, *J. Org. Chem.*, 25 (1960) 1198.
7 I. B. John, E. A. McElhill and J. O. Smith, *Ind. Eng. Chem. Prod. Res. Develop.*, 1 (1962) 2.
8 W. R. Jones and W. F. Hady, *NASA TN D-6251* (1971).
9 H. Zimmer, O. Homberg and M. Jayawant, *J. Org. Chem.*, 31 (1966) 3857.
10 C. Eaborn, *Organosilicon Compounds*, Academic Press, 1960, New York.

TASK III

DEPARTURE FROM PHASE EQUILIBRIUM DURING BOILING

Principal investigator: Joel Weisman, Professor of Nuclear Engineering

Summary

Under this project, the initiation of boiling on metal surfaces during pressure transients was investigated. The data were obtained by a new technique in which light beam fluctuations and a pressure signal were simultaneously recorded on a dual beam ocilloscope. The technique was shown to provide essentially the same results as obtained by high speed photography.

The investigation was primarily conducted with partially degassed water. Under these conditions, it was found that, for water between 90-150°C, the wall superheat required to initiate boiling during a rapid pressure transient was significantly higher than required when the pressure was slowly reduced. The result is explained by assuming a finite time is necessary for vapor to fill the cavity in which the bubble originates. Approximate calculations of this time delay are in rough agreement with the experimental observations.

During the last month of this project, considerable effort was devoted to analysis of the data and its presentation in a usable form. The information has been incorporated into a paper entitled "The Initiation of Boiling During Pressure Transients" which was presented at the ASME Meeting in Detroit (November, 1973). A copy of this paper is attached. A condensed version of this paper has been accepted for publication in the ASME Journal of Heat Transfer.

Efforts were made to extend the experimental technique developed for study of water boiling to the study of the boiling of Freon 113. Unfortunately, these efforts were largely unsuccessful. Boiling tended to start at the ends of the ribbon rather than at the area viewed by the light beam. No fully satisfactory experimental procedure was devised for use with Freon 113.

The Initiation of Boiling During Pressure Transients

J. WEISMAN G. BUSSELL I. L. JASHNANI T. HSIEH

ABSTRACT

The initiation of boiling of water on metal surfaces during pressure transients has been investigated. The data were obtained by a new technique in which light beam fluctuations and a pressure signal were simultaneously recorded on a dual beam oscilloscope. The results obtained agreed with those obtained using high speed photography.

It was found that, for water temperatures between 90-150°C, the wall superheat required to initiate boiling during a rapid pressure transient was significantly higher than required when the pressure was slowly reduced. This result is explained by assuming that a finite time is necessary for vapor to fill the cavity at which the bubble originates. Experimental measurements of this time are in reasonably good agreement with calculations based on the proposed theory. The theory includes a new procedure for estimating the coefficient of vaporization.

NOMENCLATURE

a	interfacial area, cm^2
A	area available for diffusion, m^2
b	parameter of Weibull distribution
C	coefficient of vaporization
F	probability distribution function
G	free energy, dyne cm
h_{fg}	enthalpy change on evaporator, cal/gm
J	mechanical equivalent of heat
K	constant
m	parameter of Weibull distribution
M	molecular weight, g/gm mole
n	number of active nucleation sites
n"	number of active nucleation sites per unit area, $(cm^2)^{-1}$
N	number of gm-moles
p	probability
P	pressure, mm Hg.
r	radius of cavity, cm
R	gas constant, dyne cm/°K g mol
S	area of heated surface, cm^2
t	time, sec
t'	boiling delay time, sec
T	temperature, °K
V	volume of cavity
W	diffusion rate, gm/sec
z	stochastic variable
δ	thickness of superheated liquid layer, cm
θ	parameter of Weibull distribution
μ	mean of distribution
ρ	density, g/cc
σ	standard deviation
σ'	surface tension, dyne/cm

SUBSCRIPTS

avg	mean or average value
g	inert gas
L	liquid
sat	saturation
T	total
V	vapor
w	wall

INTRODUCTION

An absolutely pure liquid in a container which provides no surface cavities can sustain an appreciable tension [1]. When the liquid is subjected to a transient pressure which falls below its saturation pressure, boiling will be delayed providing the limiting tension is not exceeded. The probability of a critical bubble nucleus originating within the liquid is low and may be computed by an expression due to Volmer[2]. This phenomenon is the basis for the operation of the "bubble chamber".

The limiting tension for water, which has been determined by Briggs[1], is far in excess of that at which boiling normally begins. Any nucleation within the bulk of the liquid under such conditions is assumed to occur due to the presence of small suspended particles or gas bubbles. By use of this assumption, depressurization transients have been modeled by Hunt[3] and Edwards[4] among others. To fit available blowdown data, Edwards found it necessary to assume that there was a delay between saturation and the time a bubble first appeared. This would appear to be in agreement with Hooper and Abdelmessah's[5] experimental observation of 4 to 8 millisecond delays before the appearance of the first bubble in the liquid during a rapid depressurization.

In most situations, boiling originates on the container walls. It is generally assumed, following a suggestion of Harvey[6], that undissolved gas bubbles entrapped in reentrant cavities on the container surface provide the necessary nucleation sites. The available work on surface nucleation is well summarized by Fauske[7].

Boiling transients in which boiling originated on the container wall have been studied by several investigators. Johnson et al[8] examined boiling on the surface of metal ribbons subjected to an exponentially increasing heat flux. They found that the first vapor bubbles appeared at a superheat which was considerably in excess of that required at steady state conditions. They indicated that the time at which the first bubble appeared could be roughly correlated (within 40%) with the time required to heat a thin layer of liquid (thickness of the radius of a bubble which will remain

on the surface in unstable equilibrium) adjacent to the ribbon.

In a depressurization transient, a delay which was due to the time necessary to heat liquid adjacent to the boiling surface would not be observed. Madhaven and Mesler (9), who studied boiling on the surface of a 10 cm diameter aluminum plate during very rapid depressurization (by diaphragm rupture) saw no delay. They found a few bubbles appeared immediately (within 20 μ sec). In contrast to this work, the examination of small metal areas during rapid depressurization by Kenning and Thirunavukkarusu (10) indicated very sparse nucleation. Their examination of the number of nucleation sites on small metal plates led to non-reproducible results. To obtain a large number of sites and reproducible results they had to use specially prepared teflon coated surfaces.

The studies of Kenning and Thirunavukkarusu may be an indication of a stochastically varying delay in bubble nucleation on metal surfaces. This would appear to be contradicted by the results of Madhaven and Mesler. However, we know from bubble chamber experience that very substantial delays in surface boiling can be obtained. In view of these apparent inconsistencies, further investigation of boiling delays during depressurization was deemed appropriate.

EXPERIMENTAL APPROACH

Studies of bubble initiation and growth are generally carried out by use of high speed photography. Since such experimenta are cumbersome, an alternative procedure has been devised. The approach used is based on a scheme originally devised by Ram (11) for stochastic analysis of nucleate boiling. Ram observed that the appearance of bubbles on the surface of a filament caused intensity fluctuations in a light beam passing over the surface. In this investigation, the first appearance of these fluctuations was used to indicate the initiation of boiling.

The apparatus developed for these tests is shown in Fig. 1. The degassed water under study is contained in a 3 in. x 1-1/2 in. glass cross. Glass plates covering the ends of the 1-1/2 in. arms of the cross allow a light beam to traverse the cross. Stainless steel flanges are affixed to the ends of the 3 in. arms. Piping from one of these flanges connects the system fluid to a mercury seal. Pressure transients are produced by rapid acting solenoid valves which connect the gas above the mercury seal to a gas supply or a low pressure chamber. The rate at which the pressure falls is controlled by needle valve placed in the line leading to the low pressure chamber.

Immersion heaters, which were inserted through the stainless steel flanges, allowed the system fluid to be heated to the desired temperature. To minimize the nucleation occurring on the heater surfaces, the fluid was heated to a level above that desired. The heaters were then turned off and the system allowed to cool to the desired temperature.

The boiling surface studied was a 3/16 in. x 10-1/2 in. long nichrome ribbon, placed along the horizontal axis of the cross. The ribbon had a surface finish with a roughness of ∿70 microinches. The collimated light beam was focused along a 1 in. section of the ribbon and alligned with the slot of a photomultiplier tube. Connection to a battery with variable taps allowed the ribbon to be heated at several rates.

The system pressure was measured by a Statham thin film strain gage pressure transducer (model PA 826-100). After appropriate amplification, the pressure signal was fed to one of the inputs to a dual beam oscilloscope. The output of the photomultiplier tube was fed to the second input of this same oscilloscope. The data for each run were obtained by a recording camera mounted on the oscilloscope.

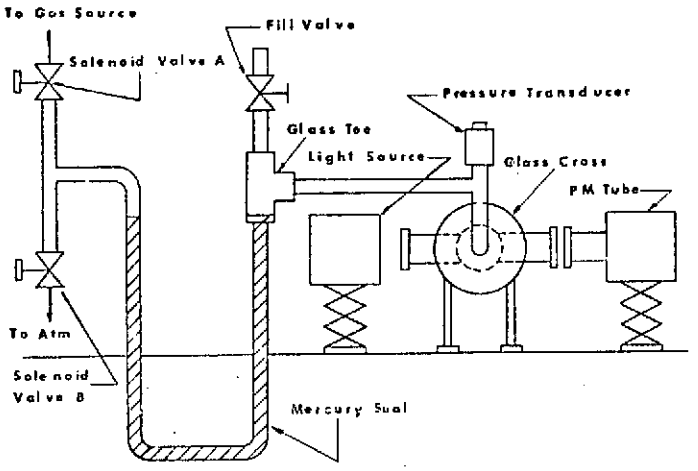

Fig. 1 Experimental Apparatus

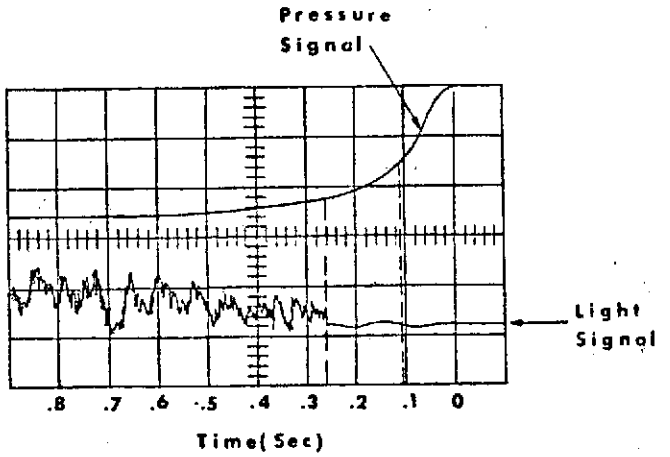

Fig. 2 Typical Oscilloscope Trace

A typical set of oscilloscope traces is shown in fig. 2. The onset of light beam fluctuations, indicating the onset of boiling, is readily correlated with the pressure signal. The upper and lower limits of the pressure signal correspond to the system pressures existing when the pressure above the mercury seal equals the high and low pressure sources, respectively. The known scope sweep time sets the time interval per abscissa division.

EXPERIMENTAL RESULTS

The first series of tests were carried out with the nichrome ribbon unheated. The experiments were initiated at ∿35 psia and the pressure reduced at rates ranging from 65 psi/sec to 4 psi/sec. These pressure reduction rates are to be regarded as approximate average rates since, as can be seen from Fig. 2, the pressure fall rate at the beginning of the transient was considerably higher than that attained at the end of the transient. Data taken initially were found to vary with operating time. After approximately 5 hours of operation, a stable surface appears to have been obtained since no further operating time effects were observed.

The data obtained in these first series of tests, after stable operation was attained, are illustrated in Fig. 3. All points shown are the averages of 3 to 5 observations. The results are expressed in terms of the wall superheat observed at the onset of boiling. Since the ribbon was not cooled until boiling began, its temperature was that of the water. The wall superheat is then the difference between the initial water temperature and the temperature corresponding to the saturation pressure at which boiling began. It is seen from Fig. 3 that the superheat required to initiate boiling increases as the rate of pressure reduction increases. This is not what one would expect if there were no delay in bubble formation.

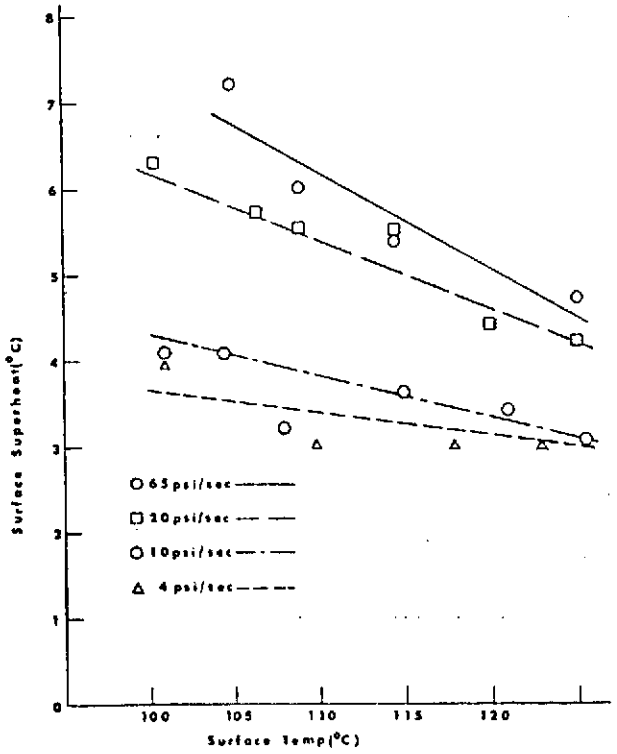

Fig. 3 Wall Superheat Required to Initiate Boiling on Unheated Ribbon.

The superheats obtained at the lower pressure reduction rates approach a single curve. This is to be expected since the superheats observed at the lowest pressure reduction rates can differ only slightly from the steady state values. Hsu (12) has shown that, at steady state conditions, the superheat for initiation of boiling may be computed from

$$T_w - T_{sat} = \frac{8\,\sigma'\,T_{sat}\,K}{J\,h_{fg}\,\rho_v\,\delta} \qquad (1)$$

where $K = 1.6$ and δ is the thickness of the superheated liquid layer. The superheats obtained at the 4 psi/sec pressure reduction rate are well correlated by Equation (1) with $\delta = 4.9 \times 10^{-4}$ in. This same value of δ correlates the data Yaglov et al (13) obtained for the initiation of boiling on a stainless steel surface at temperatures below 80°C. The superheats at the lowest pressure reduction rate were therefore taken as a close approximation of the steady state values.

A second series of tests were performed in which the nichrome ribbon was heated electrically to provide a surface heat flux of 11,000 Btu/hr.ft^2. To use this data, it is necessary to determine the nichrome ribbon temperature as a function of heat flux and water temperature. This was accomplished by very slowly reducing the system pressure until boiling was observed. The inception of boiling was assumed to occur at the steady state superheat determined in the previous tests. The heated ribbon temperatures are then the observed saturation temperature plus the steady state superheat.

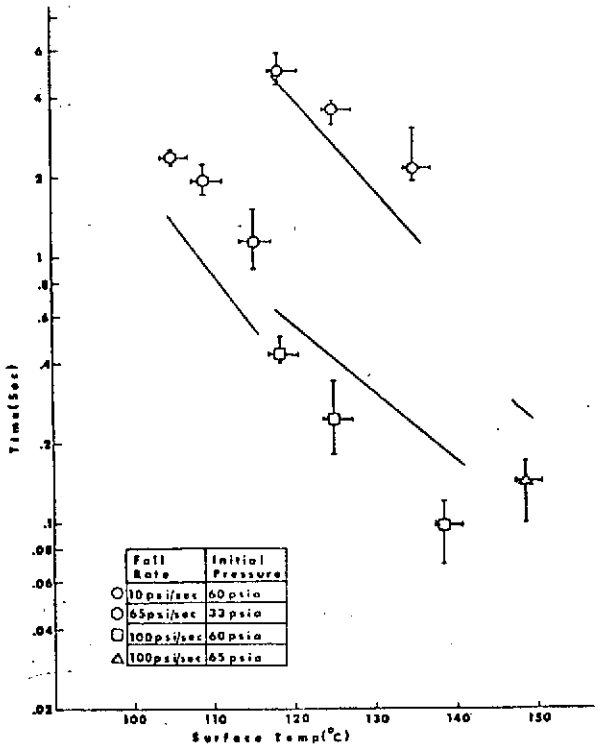

Fig. 4 Time to Onset of Boiling After Initiation of Pressure Transient

Comparison of the wall superheats obtained for several pressure reduction rates with the unheated ribbon showed no consistent pattern. At approximately the same pressure reduction rates, higher wall superheats were observed in the electrically heated tests.

A pattern is observed if the time from transient initiation to boiling is examined. It may be expected, and confirmed by Fig. 4, that appreciably longer times are required for the lower pressure fall rates. Most of this increase is due to the time required for the pressure to reach the level at which boiling would begin under steady state conditions. However, when we subtract this time from the time at which boiling is actually observed, we find (see Fig. 5) that there is an increasing delay in initiation of boiling as the pressure fall rate decreases. The delay time shown in Fig. 5 is the difference between the time light beam fluctuations were observed and the time the pressure reached the level at which steady state boiling was expected. The observed delay times ranged from a high of 1.6 seconds to a low of 65 miliseconds. Note that the runs at the highest and lowest pressure fall rates shown in Figs. 4 & 5 used a heated ribbon while the run at the intermediate rate used an unheated ribbon.

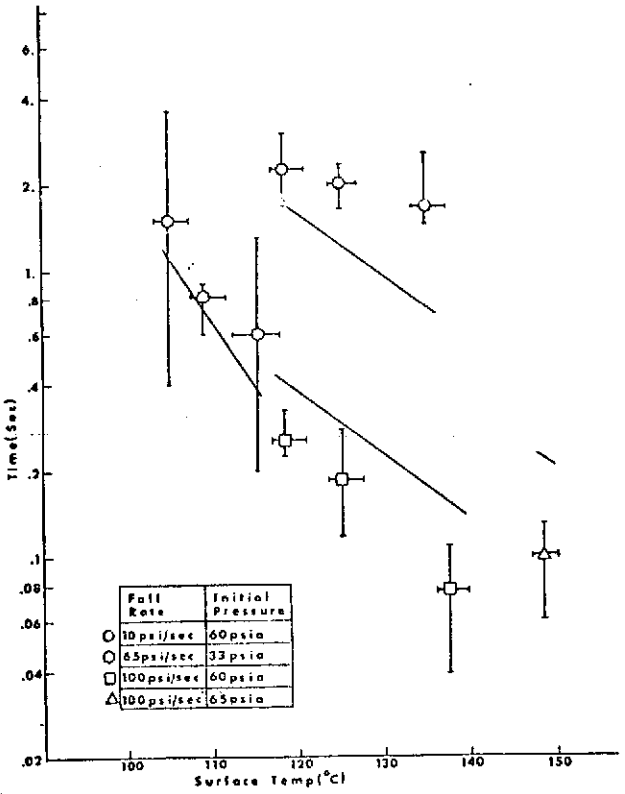

Fig. 5 Boiling Delay Time

VALIDITY OF EXPERIMENTAL APPROACH

Since the experimental method used here does not depend on direct visual observation of the boiling process, it was necessary to establish that visual observation would yield the same result. To do so, the experiment at the pressure fall rate of 100 psi/sec and ribbon temperature of 126°C was repeated while observing the results with high speed photography.

Films of the process were obtained using a Fastex motion picture camera operating at 1500 frames/sec. An initiation signal allowed synchronization of the photographs with the oscilloscope pressure signal trace. Analysis of the photographs indicated that boiling began 0.26 seconds after initiation of the transient. This corresponds to 0.185 seconds delay after the steady state superheat was attained. These times compare to an average of 0.25 seconds to boiling and 0.17 seconds delay obtained by the light beam technique. The light beam technique would thus appear satisfactory for the range of delay times investigated here.

The films of the boiling process indicated that, once a bubble appeared, approximately 4 msec was required for its growth. The light beam signal obtained from a single bubble at its maximum size was approximately 3-4 times the minimum amplitude which could be detected. Thus the reported delay times for the 100 psi/sec run will be approximately 1-1.5 msec longer than the true delay time. This is not of significance for any but the shortest delay time obtained. However, some revision of this technique would be required if substantially shorter delay times were to be observed.

Since the temperature of the electrically heated ribbon was inferred from the conditions at which steady state boiling occurred, some error may have been introduced here. The assumption that the superheat required to initiate boiling is independent of the initial system pressure is not entirely correct (14). This can introduce an error of a few °C into the estimate of the wire temperature. However, the pressure at which steady state boiling began was observed experimentally. Since this pressure was that used as the basis for obtaining delay times, this procedure would not affect the computed delay times.

The accuracy of the transient pressure measurements must also be considered. A Statham Model PA 82(;)00 thin film strain gage transducer, designed for high frequency response, was used. This pressure transducer has a limited temperature range and thus it was necessary to locate it in a cool region. The transducer was therefore connected to the piping rather than directly to the steel flange. Hence, it may be postulated that the difference in pressure between the transducer and the nichrome ribbon varied during the transient. Such a situation could arrise if a gas pocket were present in the glass cross. Care was taken to see that such a pocket did not exist. A capillary tubing line was used to vent such pockets after filling and degassing and no free surface was present in the glass cross during the experiments.

The presence of a bubble on the face of the transducer would have affected the pressure reading. A hypodermic needle was used to fill the transducer cavity and the tranducer was connected to a completely filled line thus eliminating any possibility of a bubble. The system configuration was such that no vapor bubble generated during the experiment could enter the line to the transducer.

It may be postulated that, if boiling occurred in the liquid between the nichrom wire and pressure transducer, an additional pressure gradient could have been introduced. While such boiling did occur in the experiments with the unheated nichrome ribbon, this was not the case when the nichrome ribbon was heated. In these runs, boiling was first observed on the ribbon. Hence, no additional pressure gradient can be postulated for these runs which provide the majority of the delay time data.

While the above would appear to eliminate the major arguments which might suggest that the inferred surface temperatures or pressures are in error, they do not furnish conclusive proof. It could be argued that another, but unknown, error led to an incorrect temperature or pressure inference. The only conclusive proof of the existence of a time delay is the measurement of such a time delay under conditions essentially independent of temperature and pressure inferences. Experiments in which the system pressure dropped to its lowest value at some time prior to the onset of boiling provide this proof. Fig. 6 reproduces the oscilloscope traces obtained in such a run. It is seen that the pressure reached its final level approximately 0.28 seconds before the light beam trace shows any indication of boiling. We must therefore conclude that the boiling delay was at least 0.28 seconds. Several such runs were obtained. This delay is not dependent on a knowledge of the exact level of temperature or pressure. The results of these runs were in agreement with the remainder of the data.

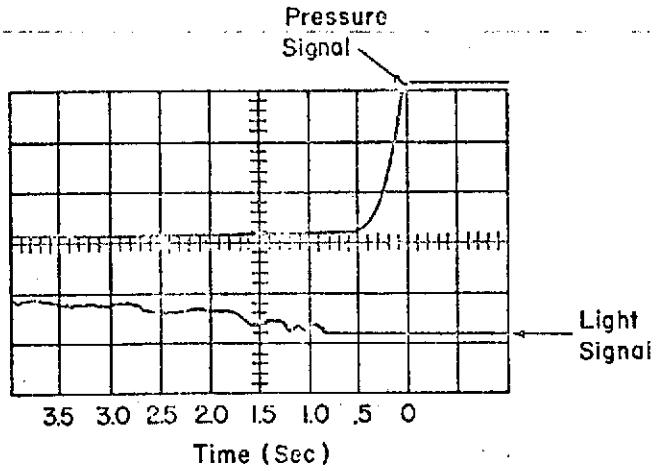

Fig. 6 Oscilloscope Trace Clearly Showing Delay Time.

On the basis of the foregoing observations it was concluded that the delay times observed were valid. An explanation of the observed delays was therefore sought.

It should be recognized that the relatively long delay times observed are due to the special experimental conditions. It has previously been noted that the rate of pressure full at the end of the transient was substantially below the average pressure fall rate. Thus, while the delay times at the lowest pressure fall rate were appreciable, the surface was maintained at a superheat which was at most only a few degrees above the steady state value. In most transients of practical interest, pressure fall rates will be substantially higher than used in these tests. Substantially shortened boiling delay times are therefore to be expected.

ANALYSIS OF NUCLEUS GROWTH IN SURFACE CAVITY

As previously observed, it is generally accepted that nucleation begins at a small vapor bubble at the lower end of a surface cavity. As the system pressure is reduced, the vapor bubble begins to grow. When the bubble has filled the entire cavity, it is observable on the surface. Any delay in the appearance of a bubble on the surface must therefore be attributed to the time required for the vapor bubble to grow and fill the entire cavity.

The postulated bubble behavior is consistent with the pressure-temperature history model proposed by Fabic (15) and Holtz (16). When boiling occurs from a reentrant surface cavity, the incipient superheat can be obtained from

$$P_v - P_L = \frac{2\sigma'}{r} \qquad (2)$$

Since the incipient superheat for the system investigated was only about 3°C at atmospheric pressure, $(P_v - P_L)$ is approximately 1.9 psi. If a higher pressure P_L' is now applied to the system, the cavity will be flooded if

$$P_L' \geq \frac{2\sigma'}{r} + P_v + P_g \qquad (3)$$

For degassed water at 100°C, P_g will be quite low and the right hand side of Equation (3) will equal about 16.6 psi. Hence, application of a system pressure of 60 psia, as done in the present experiments, will cause reflooding of the cavity.

The difficulty of completely degassing water is well known and hence some air will be present in the vapor originally in the cavity. Application of the 60 psi system pressure will lead to condensation of nearly all the vapor but retention of the air in a small gas bubble at the base of the cavity. Diffusion of air from this bubble into the liquid will gradually occur. However, over the short periods during which the high system pressure is maintained, the amount of diffusion is low. The small gas bubble is then available to serve as a nucleus for vapor growth on the next pressure reduction.

Inertia, heat transfer and mass transfer rates determine bubble growth. However, since the bubble nucleus is surrounded by high conductivity metal, heat transfer rates should be high. Further, since the rate of nucleus growth is low, inertia effects should not be limiting. It will therefore be assumed that rate of bubble growth is determined by the rate of mass transfer across the vapor-liquid interface. As the pressure drops, the gas in the bubble expands, the water vapor pressure drops below the equilibrium value and diffusion occurs. Knudson's diffusion equation gives, $\frac{dW-}{dt}$, the rate at which vapor molecules impinge on the interface surface, as

$$\frac{dW-}{dt} = \sqrt{\frac{M}{2\pi R}} \frac{P_v A}{\sqrt{T_v}} = .0583\ P_v A \sqrt{\frac{M}{T_v}} \qquad (4)$$

and the rate at which liquid molecules impinge on the interface, $\frac{dW+}{dt}$, as

$$\frac{dW+}{dt} = 0.0583\ P_L A \sqrt{\frac{M}{T_L}} \qquad (5)$$

However, not all molecules impinging on the surface actually penetrate the interface. Introduction of a coefficient of vaporization (14), or condensation, C, representing the probability that a molecule will penetrate the interface and not be reflected gives us the net rate of transfer as

$$\frac{dW}{dt} = 0.0583\ CA \sqrt{\frac{M}{T}} (P_L - P_V) \qquad (6)$$

if $T_L = T_v = T$.

If we take the number of moles of air in the cavity as N_g, the moles of water as N_v, and the total pressure in the cavity as P_T, then

$$P_v = \left(\frac{N_v}{N_g + N_v} \right) P_T \qquad (7)$$

and we may write

$$\frac{dN_v}{dt} = k' \left(P_L - \left(\frac{N_v}{N_g + N_v} \right) P_T \right) \qquad (8)$$

where $k' = 0.0583\ CA/\sqrt{M/T}$
In general, P_T will be a complex function of t and the time required to fill the entire cavity must be obtained by a numerical integration of Equation (8). However, for the special case of a step change in P_T, with fluid temperature and A held constant, we have

$$t = \frac{1}{k'} \left\{ \frac{N_a}{(P_L - P_f)} \ln(N_a P_L + (P_L - P_f)N_v) + \frac{1}{(P_L - P_f)^2} [N_a P_L + (P_L - P_f)N_v - N_a P_L \ln(N_a P_L + (P_L - P_f)N_v)] \right\}_{N_{v_o}}^{N_{v_f}} \qquad (9)$$

where P_f is the final pressure in the cavity and $N_{v_f} = \left(\frac{P_f V}{RT} \right)$.

Numerical evaluation of Equation (8) requires an estimate of: the ratio of A to cavity volume, the fraction of inert gas present before pressurization, and the vaporization (condensation) coefficient. This latter quantity can be determined by an extension of the theory used for estimating the probability of thin film rupture providing the effect of steric hinderance is negligible.

The fluctuation in the thickness of liquid surface films may be caused by mechanical or thermal variations. If the free energy of the film in the normal state is G_o, and if G_1 is the free energy of the surface after some fluctuation, then the probability, p_1, of such a fluctuation is given by Scheludko (17) as

$$p_1 = K_1 \exp \left[\frac{G_o - G_1}{kT} \right] \qquad (10)$$

Jashnani (18) used this expression to determine the rupture probability of thin films.

The same reasoning may be applied to rupture of surfaces. However, the free-energy change involved is due to the change in surface area, Δa, rather than thickness. Hence

$$G_1(t) - G_o(t) = -\Delta G = \sigma \Delta a \qquad (11)$$

Equation (10) then becomes

$$C(A)dA = (K_2)\ e^{-\frac{\sigma' \Delta a}{kT}}\ da \qquad (12)$$

The variation in surface tension due to dynamic conditions is unknown and is therefore neglected.

To determine the value of K_2, we normalize the frequency function and obtain

$$C = \frac{e^{-\frac{\sigma' \Delta a}{kT}}}{\int_o^\infty e^{-\frac{\sigma' \Delta a}{kT}}\ d\Delta a} \qquad (13)$$

Since all fluctuations having changes in free energy which correspond to area changes greater than Δa will result in rupture, then

$$C = \frac{\int_{\Delta a}^\infty e^{-\frac{\sigma' \Delta a}{kT}}\ d\Delta a = e^{-\frac{\sigma' \Delta a}{kT}}}{\int_o^\infty e^{-\frac{\sigma' \Delta a}{dT}}\ d\Delta a} \qquad (14)$$

For water, the bond length between O and H atoms is 0.958 °A and the angle between bonds 104.45°. Hence, the total length of the molecule is less than 2°A. If the gas molecule is assumed to depress 2-3 molecules near the center of the depression area where it strikes, then it is reasonable to assume the shape shown in Fig. 6 for the surface before condensation. The actual change in surface will be smooth and the figure shows sharp corners merely to facilitate calculations. The gas molecules are assumed to approach normal to the surface. Gas molecules with a small kinetic energy will bounce back. An energetic molecule will depress the surface and create a hole at the center of the depression. The gas molecule then becomes part of the liquid and the surface moves to its original shape which is stable.

The change in area will be the difference between the area shown in Fig. 7 and the original area. We obtain

$$\Delta a = \pi(29.5 - 16) = 13.5\pi = 42.3\ A^{\circ 2} \qquad (15)$$

assuming the above area is the statistical average area for a gas molecule striking at any angle. This lends to

$$\Delta G = 42.3 \times 10^{-16}\ \sigma' \qquad (16)$$

For water temperatures around 100°C, we obtain C ≈ .01. The work of Johnstone and Smith (19) indicates that, for water at exposure times in excess of 100 msec, C ≈ .02. This is considered quite good agreement with the present estimate since an error of only 15% in the value of (Δa) would account for the difference in values of C.

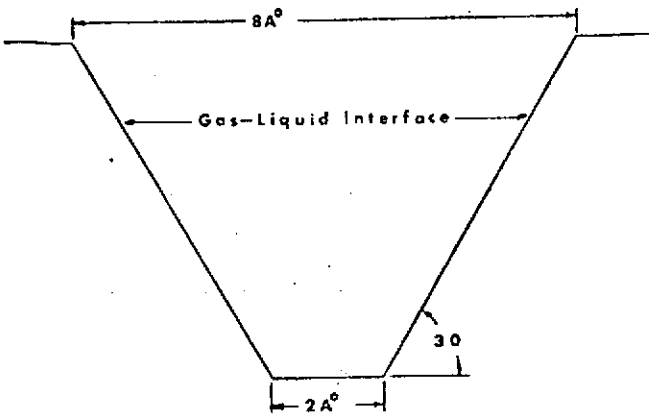

Fig. 7 Surface Area Depression Caused by Molecule Striking Interface

COMPARISON OF THEORY AND RESULTS

If the Equation (14) is used for evaluation of C, it is now possible to compute the rate of bubble growth for any given pressure transient by use of Equation (8) in finite difference form. It was arbitrarily assumed that before the overpressure was applied the air partial pressure in the cavity was .02 atm*. The total pressure inside the bubble was assumed to vary between the system pressure less a small differential at the beginning of the transient and the system pressure plus an increment, equivalent to the equilibrium superheat, at the end of the transient. A search was then made for a volume to surface area ratio (V/A) for the cavity which would allow prediction of the experimental results. The solid lines of Figs. 4 and 5 show the results of these calculations using V/A = .003 cm. (This corresponds to a cylindrical cavity .003 cm in depth.) It is seen that reasonable agreement is obtained with the theory correctly predicting all the observed trends.

It will be observed that the theory tends to underpredict the delay times of the 10 psi/sec and 65 psi/sec while correctly predicting the delay times for the 100 psi/sec data. This is understandable since the 100 psi/sec data were obtained at an average superheat of about 15°C while the 10 psi/sec data were obtained at a superheat of about 10°C and the 65 psi/sec data at ∿7 °C. superheat. The higher superheat for the 100 psi/sec data may be expected to activate more nucleation sites and thus lower the observed delay time. Effectively, a lower value of V/A should probably be used for the higher superheats.

The experiments of Kenning and Thirunavukkarasu (10) are the closest to these conducted here. If the present theory is used to estimate the bubble delay time in their experiment (after appropriately allowing for the effect of increasing superheat on the effective V/A) delay times of the order of 7-11 msec are obtained. A stochastically varying delay time of this order of magnitude would explain their observations.

The pressure-time history approach also offers a possible explanation for the results of Madhaven and Mesler (9). In these experiments, water was degassed by boiling at one atmosphere. After allowing the water to cool, the pressure was suddenly reduced. Cavities which were too small to serve as nuclei during the boiling at one atmosphere would remain full of air. If the pressure transient produced a superheat sufficient to activate these small cavities, some bubbles would be observed on the surface almost immediately. In both the present experiments and those of Kenning and Thirunavukkarasu (10) the high overpressure which was initially applied may be expected to cause flooding of the available nucleation sites. Delays in the initiation of boiling may therefore be expected.

STOCHASTIC NATURE OF BOILING INITIATION

The stochastic nature of the boiling process has been acknowledged by numerous investigators. Boiling initiation may therefore be expected to be a stochastic phenomenon. The high speed photographs taken of the process indicate this to be the case. The appearance of the first bubble does not always occur at the same site and there is appreciable variability in the delay time at any given site. These observations agree with those of Kenning and Thirunavukkarasu (10). As may be seen from Figs. 4 and 5, the variability in bubble behavior is reflected in the delay times measured for the assemblage of sites observed in these experiments. The vertical lines through each of the data points represent the total range of observations for a particular set of conditions. In most cases, the variation observed is far beyond the ascribable to measurement errors.

Computation of the variance in boiling delay time for those conditions where 9-12 replications were undertaken indicates that σ/μ is in the range of 0.24-0.32. Similar results are obtained by considering the data at the 100 psi/sec pressure reduction rate as one group and the data at 10 psi/sec in another group. When all the data taken with the heated ribbon are pooled, the sample σ/μ is computed as 0.282 giving 0.285 as an unbiased estimate of σ/μ.

The Weibull distribution (20) has been found useful in correlating a variety of physical phenomena. The Weibull distribution function has the form

$$F = 1 - \exp\left[-(z-b)^m/\theta\right] \qquad (17)$$

where b, m, and θ are parameters to be determined. If we let $z = t'/t'_{avg}$, and utilize the work of Dubey (21) to set b, m and θ so that σ for the distribution is that of the observed data, μ = 1, and the probability of a delay time less than zero is zero, we obtain

$$F = 1-\exp\left[-(t'/t'_{avg})^{3.95}/1.48\right] \qquad (18)$$

Comparison of this function with the observed data distribution in Fig. 8 shows good agreement. The quantity F is the probability that the delay time is less than t'.

*Values of .01 to .05 atm. worked equally well provided V/A was appropriately adjusted.

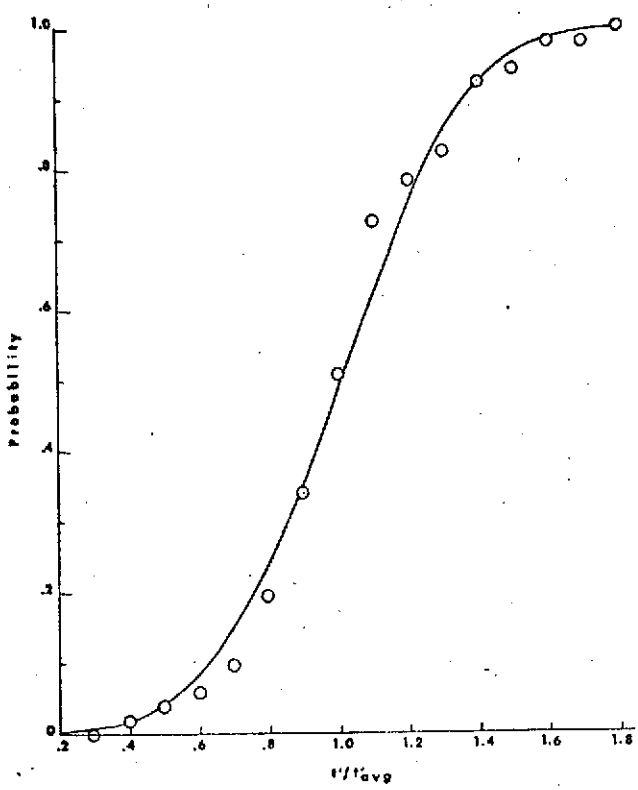

ig. 8 Distribution of Delay Times

The delay times which were observed in these ests correspond to the behavior of an assemblage of ctive sites. It would be desirable to obtain the be-avior of a single site. The properties of the Wei-ull distribution make it particularly useful for this urpose. If the delay time distribution function for single site is given by

$$F' = 1-\exp[-z^m/\theta_1] \qquad (19)$$

here "F'" corresponds to the probability that the de-ay time at a single site will be less than z. If n ites are simultaneously observed, the probability F f a delay time less than z is given by $[1 - (1-F')^n]$. ence, F, is given by

$$F = 1 - \exp[-n\, z^m/\theta_1] \qquad (20)$$

he distribution F corresponds to the distribution of elay terms obtained by observing n_1 sites on the nich-ome ribbon and therefore $n/\theta_1 = \frac{1}{1.48}$. Photographs f the area of the ribbon observed indicate $n \simeq 10$ ence

$$F' = 1 - \exp\left[-\left(\frac{t'}{t'_{avg}}\right)^{3.95}/14.8\right] \qquad (21)$$

rom the work of Dubey (21) we can show that the mean f this distribution, and hence the average delay ime for a single site, would then be $n^{1/m}(t'/t'_{avg}) = .79(t'/t'_{avg})$. The standard deviation of this istribution is simply $n^{1/m}$ times the standard de-iation of the original σ obtained from Eq. (18).

It is clear that the larger the area observed, he lower the mean delay time. If the number of ctive sites per unit area is n" and the area observed s S, then Equation (20) becomes

$$F = 1 - \exp(-\, n''\, S(t'/t'_{avg})^{3.95}/14.8] \qquad (22)$$

Since increasing superheat increases n", the effect of increased wall superheat is to decrease the observed delay time. If the dependence of number of nucleation sites on wall superheat were known, values of F could be estimated if all the smaller size sites have about the same average V/A. The total number of active sites at t', which is gimen by n"F', could then be estimated.

CONCLUSION

A new technique for the study of boiling initiation has been developed. The new method again demonstrates that, under appropriate conditions, appreciable delays can be encountered in the initiation of boiling on metal surfaces. These delays can be explained in terms of the time required to fill the nucleation cavity with vapor. The observed delays are found to vary stochastically and should therefore be described in terms of a probability distribution function.

ACKNOWLEDGEMENT

The authors wish to acknowledge the financial assistance of the Lewis Research Center of the National Aeronautics and Space Administration under whose sponsorship this research was conducted. Special thanks are due to Dr. R. Graham and Dr. Y.Y. Hsu of the Lewis Research Center for their advice and encouragement.

REFERENCES

(1) Briggs, J.L., J. Applied Physics 26, 1001 (1955).

(2) Volmer, M., "Kinetics der Phasenbildung" in "Die Chemishe Reaction," Vol. 4, edited by K.F. Bonhoeffer, Leipzig, Steinkopf (1939).

(3) Hunt, D.L. "The Effect of Delayed Bubble Growth on the Depressurisation of Vessels Containing High-Temperature Water," UKAE Report AHSB(S) R. 189, United Kingdom Atomic Energy Authority (1970).

(4) Edwards, A.R., "Conduction Controlled Flashing of a Fluid and the Production of Critical Flow Rates in a One-Deimensional Syste," UKAEA Report AHSB(S) R147, United Kingdom Atomic Energy Authority (1968).

(5) Hooper, F.C., and A.H. Abdelmessah, "Flashing of Liquids at High Superheats," Third International Heat Transfer Confernce, Vol. 4, 44 (1966).

(6) Harvey, E.N., A.H. Whitely, J. Appl. Physics 18, Feb. 1947.

(7) Fauske, H.K., Reactor Technology, 15, 278 (1973).

(8) Johnson, R.A., V.E. Schrock, F.B. Selph, J.H. Lienhard, Z.H., Roszloczy, International Developments in Heat Transfer, Pt. II, p. 254, ASME (1961).

(9) Madhaven, S. and R. Mesler, "A Study of Bubble Growth on Surfaces," Fourth International Heat Transfer Conference, Vol. V., paper B 2.6 (1970).

(10) Kenning, D.B.R. and K. Thirunavukkarasu, "Bubble Nucleation Following a Sudden Pressure Reduction in Water," Fourth International Heat Transfer Conference, Vol. V., paper B 2.9 (1970).

(11) Ram, K.S., Trans of A.N.S. 12, No. 1, 301 (1969).

(12) Hsu, Y.Y., Tran A.S.M.E., J. Heat Transfer 84, 207 (1962).

(13) Yaglov, V.V. et al, Int. Chem. Eng. 10, 607 (1970).

(14) Okrent, D. and Fauske, H.K., "Transient Sodium Boiling and Voiding in Fast Reactors," Bulletin ANL/ACEA-101, Argonne Nat. Lab. (1972).

(15) Fabic, S., "Vapor Nucleation on Surfaces Subjected to Transient Heating" Report NE-64-1, Institute of Eng. Research, Univ. of California, Berkely (1964).

(16) Holtz, R.E., "The Effect of Pressure-Temperature History Upon Incipient Boiling Superheats, U.S.A.E.C. Report ANL-7184, Argonne Nat. Lab. (1966).

(17) Scheludko, A.I., Zhur. Electrochem. 61, 220 (1957).

(18) Jashnani, I.L., "Coalescence and HTU in Foam Fractionation," Ph.D. Dissertation, Univ. of Cincinnati, (1971).

(19) Johnstone, R.K. and W. Smith, "Rate of Condensation or Evaporation During Short Exposures of a Quiescent Liquid," Third International Heat Transfer Conference, Vol. II, p. 348, AIChE (1966).

(20) Weibull, W.J. , Applied Mechanics, 18, 293 (1951).

(21) Dubey, S.D., Naval Research Logistics Quarterly 14, 69.

TASK IV

EFFECTS ON NEUTRON IRRADIATION ON THE DEFECT STATE IN TUNGSTEN

Principal Investigator: John Moteff, Professor of Materials Science Engineering

Introduction

The purpose of the proposed research was to:

a) Review, collect and evaluate all available published data on the effects on neutron irradiation on the mechanical and physical properties of tungsten and tungsten-base alloys.

b) Conduct experimental investigations to determine the defect recovery behavior in neutron irradiated tungsten and one tungsten rhenium alloy, both irradiated simultaneously to a fast neutron fluence of 1×10^{22} neutrons cm^{-2}, $E_n > 1$ MeV at six temperatures lying in the range of 425 - 1000°C.

Reviews of the literature have been initiated consistent with part (a) of the proposed program. The complete review will be presented in the Masters Thesis of one of the investigators (J. Matolich). It should be pointed out however, that information on the effects of radiation on tungsten and tungsten-base alloys is quite limited and this circumstance is obvious in view of the lack of literature published on these materials. Most of the effort in the past has been performed and reported prior to 1970 with the bulk of the data still in AEC and/or NASA limited distribution reports.

Work has been completed on the subprograms:

(i) isochronal resistivity recovery studies and

(ii) isochronal hardness recovery measurements

with some preliminary work completed on Transmission Electron Microscopy.

Most of the studies on this program has been confined to the measurement of room temperature hardness and resistivity properties following high temperature anneals and it is this phase of the program that is reported herein. The data will be reported according to material category.

Tungsten

The highest melting point BCC metal is tungsten and studies on this material should be useful in the interpretation of the radiation induced property changes in metals such as Mo, Cr, Nb, Ta, V and α-Fe.

Hardness Measurements - Tungsten specimens approximately 1 mm in diameter were annealed at 1750°C for one hour in a vacuum before being irradiated in EBR-II. Irradiation temperatures were 430, 550, 700, 800, 900 and 1000°C. The specimens were irradiated in Row 7 of the EBR-II to a fast neutron fluence to approximately 1×10^{22} n cm^{-2}, ($E_n > 1$ MeV).

Following the irradiation, one specimen rod was selected from each of the six irradiation temperatures. The specimens were placed in a cutting rig and approximately 20 slices ($\sim$ 20 mil thick) were cut from each of the rods for use in both the hardness and the transmission electron microscopy studies. The samples were properly accounted for and separated into small furnace annealing rigs carefully wrapped in tantalum foil Sets of these specimen were subsequently annealed for one hour in a

vacuum of less than 5×10^{-6} torr, at thirteen separate temperatures ranging from 430° to 1940°C. Including the control samples, the number of small discs to be used in the studies on tungsten hardness studies were approximately 100 pieces. About 25 pieces were used in the TEM work.

Following the anneal treatment, the specimens were then mounted in bakelite molds and ground initially with silica carbide (600 paper). Polishing was performed in two steps, with a final 0.3 micron alumina particle polishing time of approximately 10 minutes. Knoop hardness measurements were then performed on the surface of the specimen. Approximately 5 to 10 indents were made on each. The preliminary hardness data is presented in Figure 1.

Resistivity - Detailed resistivity measurements have been completed for specimens irradiated at the six different temperatures and the data will be presented in the Figures 2A and B.

This portion of the experimental program took longer to perform than initially planned. Since it was decided that much smaller temperature intervals should be made in order to obtain a better resistivity.

Approximatley 440 separate resistivity measurements had to be made on the irradiated plus control specimens for the 27 separate temperature anneals for both the W and W-25Re specimens. Approximately four days were required to anneal and perform the

resistivity measurements for each anneal temperature. This amount of effort was considered necessary in view of the importance of the type of information which was being obtained.

Tungsten-25 Percent Rhenium

The W-25Re is a solid solution alloy and the large amount of the Re present in the alloy is shown to significantly affect the nature of the radiation induced defect configurations.

Hardness Measurements - The room temperature hardness measurements were performed in a manner similar to the case of tungsten. Figure 3 shows a plot of the room temperature hardness as a function of irradiation temperature for different anneal temperatures. This work clearly shows that a temperature of approximately 1700°C is required to anneal out all the defects.

Resistivity - The resistivity recovery behavior of the W-25Re is very different than that obtained from the case of tungsten. As shown in Figure 4, the resistivity for the three lower temperatures has increased over and above the control specimens as a result of the irradiations. This trend was expected. On the other hand, the specimens irradiated at the three higher temperatures suggests a negative resistivity compared to the control specimens. This circumstance is due to the fact that a radiation induced precipitate of a rhenium rich second phase (α-manganese phase) reduced the rhenium concentration in solution. The decrease in resistivity due to the depletion of rhenium

in solution obviously is greater than the increase in resistivity due to the formation of point defects and defect clusters, thereby resulting in a net negative resistivity relative to the control.

Summary

The two most important features of the recovery studies i.e., resistivity and hardness has been completed for the two alloys irradiated at the six different temperatures. Since the contract support is nearing termination, the final data analysis of this work will be documented in the Masters Thesis of one of the investigators. Since this thesis will be forthcoming (by the end of the calendar year) it will be assumed that the detailed description of the work performed, data generated and final analysis of the data will meet, in a large part, the committment made in this contract. In addition, it is anticipated that approximately two papers will be published on the final results of this work. The support of this NASA contract for the work performed will be acknowledged in the publications.

It should also be pointed out that the data presented in this progress report represents preliminary information and that final corrections, data reduction and subsequent analysis may change the exact effective temperatures slightly.

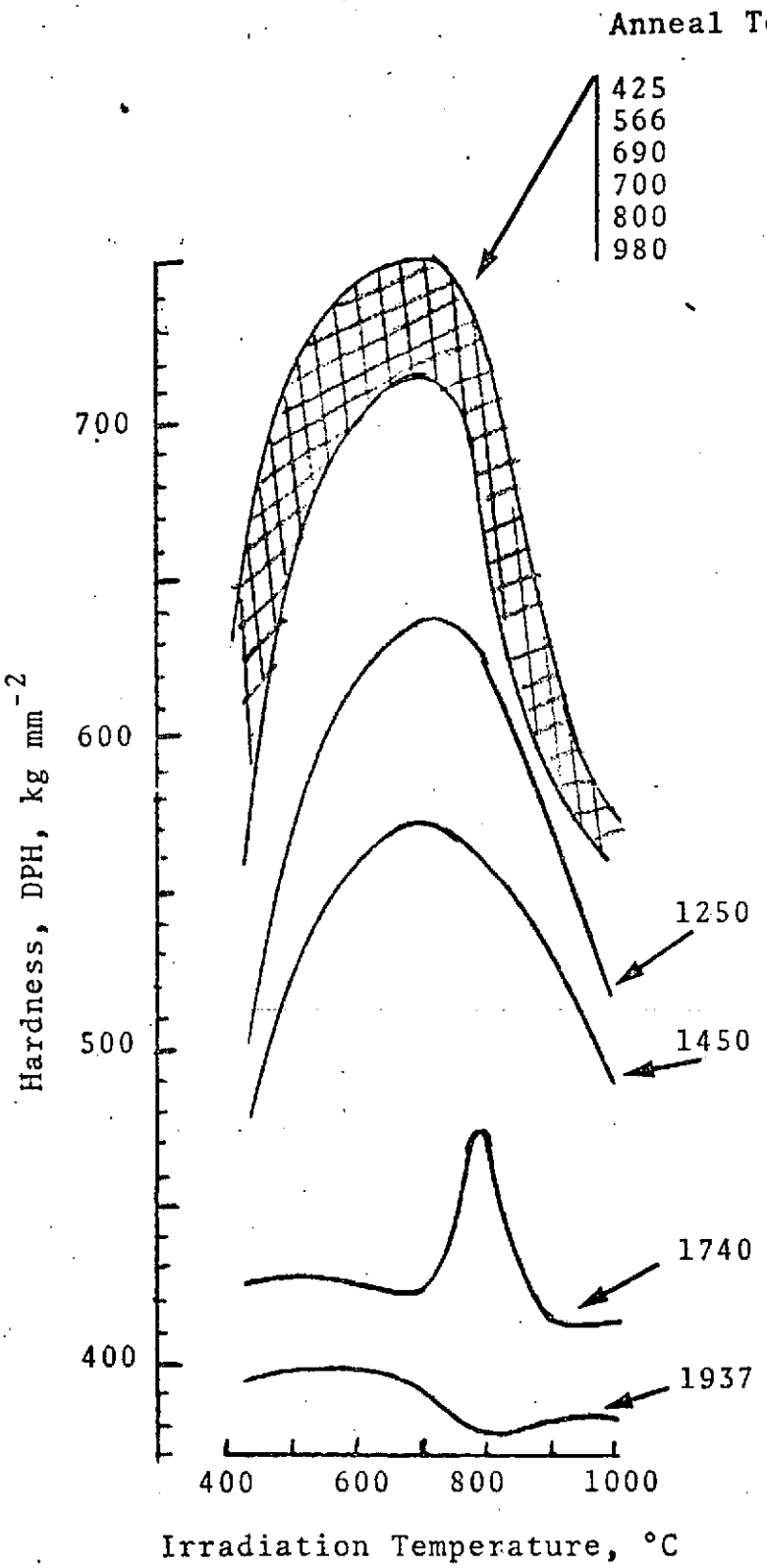

Figure 1 Room Temperature Microhardness as a Function of Irradiation for Various Anneal Temperatures (Irradiated Tungsten).

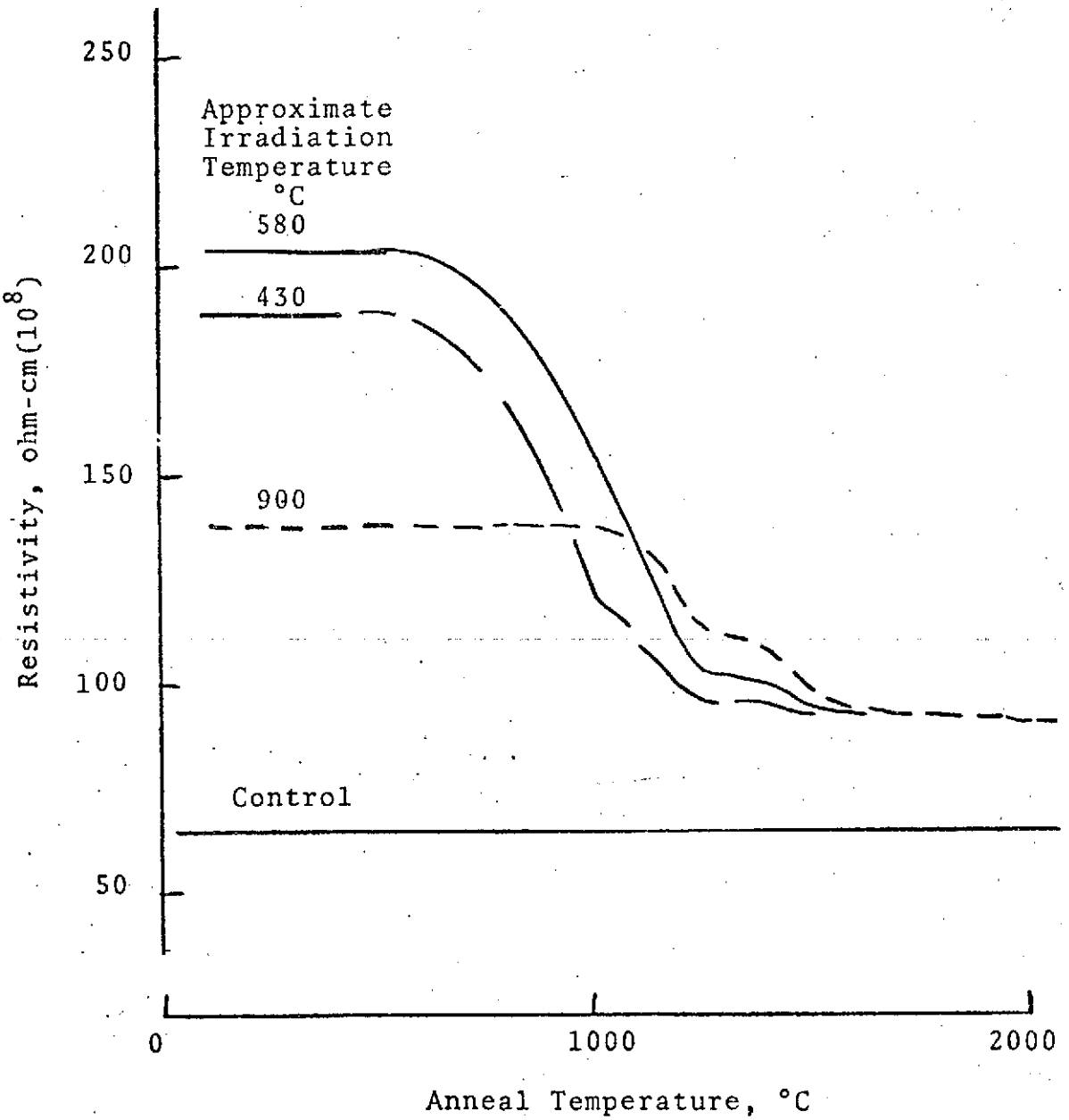

Figure 2A Recovery of Neutron Irradiation Tungsten Resistivity as a Function of Anneal Temperatures for Different Irradiation Temperatures.

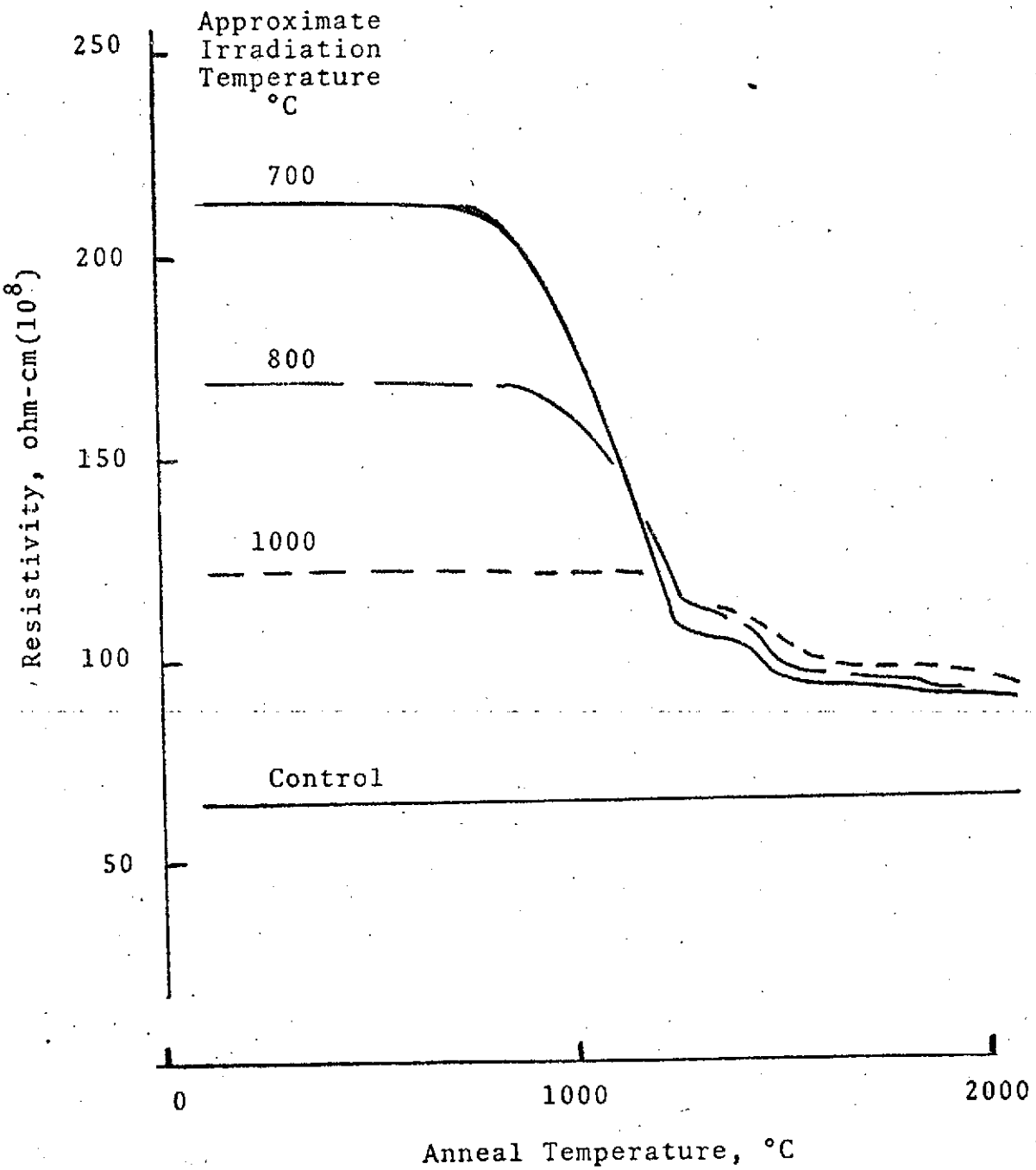

Figure 2B Recovery of Neutron Irradiation Tungsten Resistivity as a Function of Anneal Temperatures for Different Irradiation Temperatures.

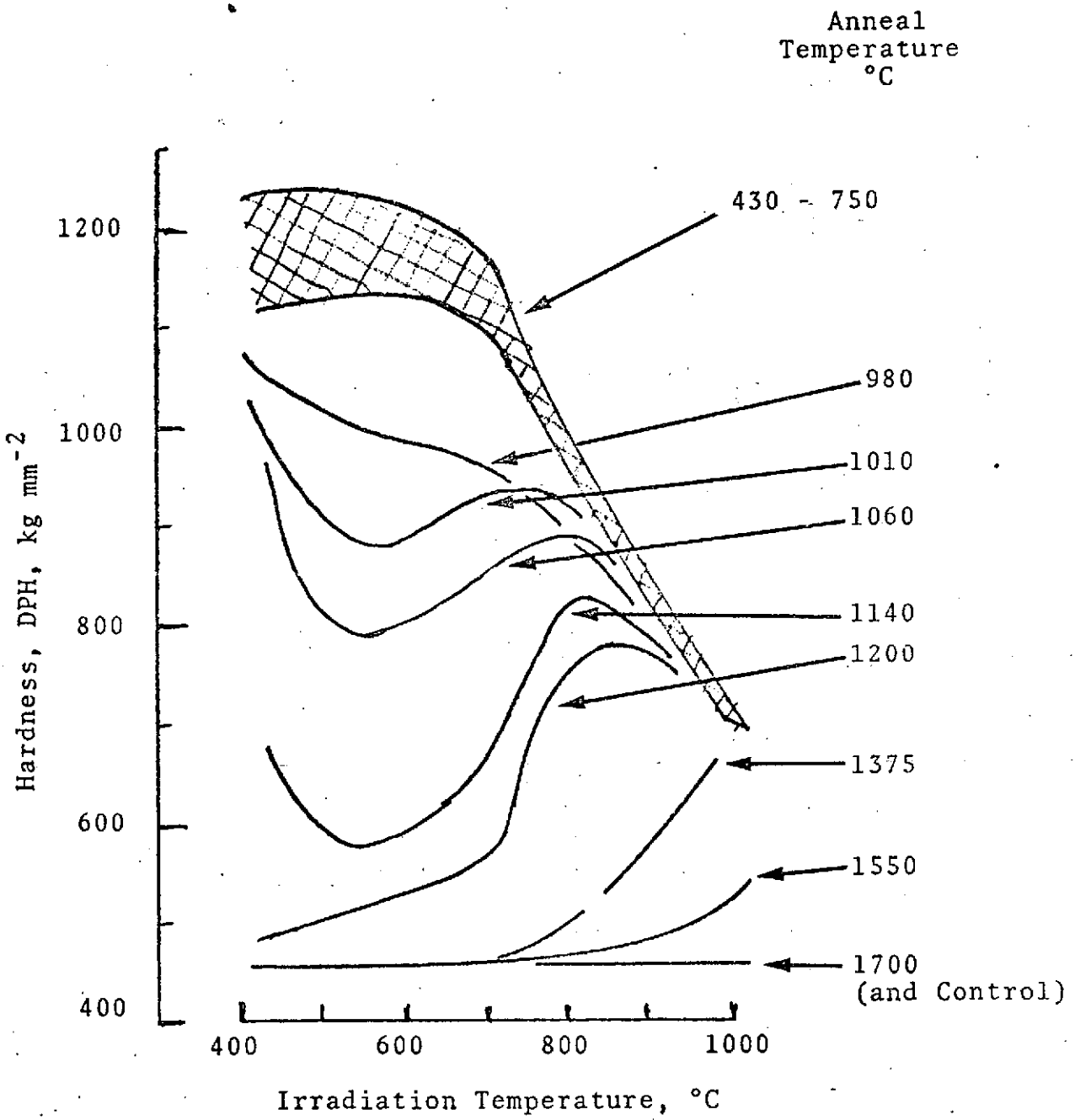

Figure 3 Microhardness of Neutron Irradiated W-25Re as a Function of Irradiation Temperature for Various Anneal Temperatures.

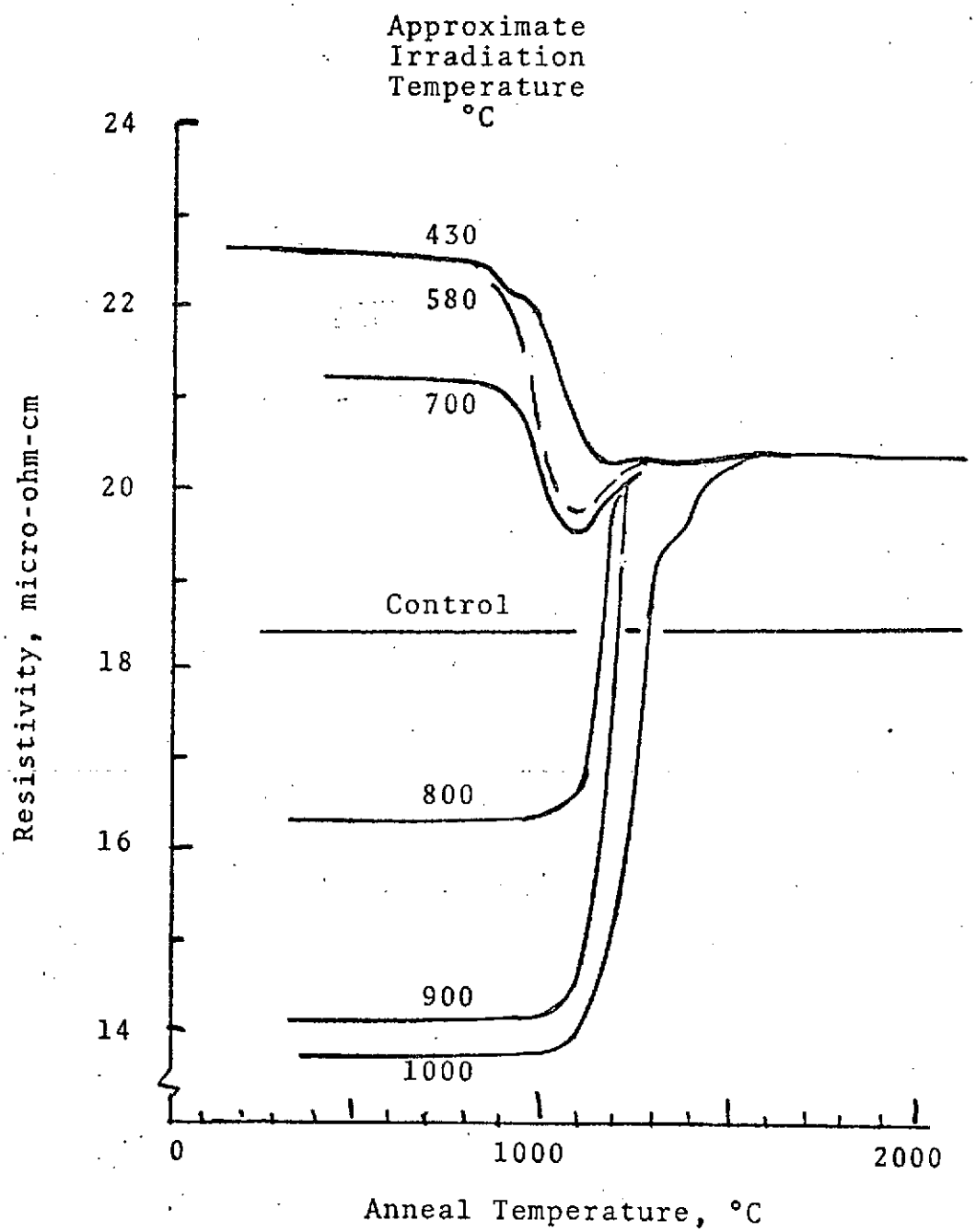

Figure 4 Recovery of the Electrical Resistivity of Neutron Irradiated W-25Re as a Function of Anneal Temperature for Various Irradiation Temperatures.

TASK V

DETERMINATION OF PHOTON RESPONSE FUNCTION OF NE-213 LIQUID SCINTILLATION DETECTORS

Principal Investigator - A. Shapiro, Associate Professor of Nuclear Engineering

I. Introduction

The objective of this work was to establish the gamma response function of a 2 inch by 2 inch NE-213 detector from incident bremsstrahlung radiation of varying maximum energies. At this time, much of the data has been accumulated, but the analysis of the data has not yet been completed. Progress has been slowed by the fact that two consecutive students assigned to the project left school suddenly to accept job offers, plus the usual type of delays associated with equipment failure. As a consequence, this report must be taken as a progress report, with the final report to be submitted at a later date.

II. Calibration of Betatron and Establishment of Incident Spectrum

For this work, the betatron of the Nuclear Engineering Laboratory served as a source of gamma radiation. Since the betatron had not been used for some time prior to this work, it was necessary to check the energy calibration. In addition, to evaluate the response of a detector, the spectrum incident on the detector must be known. To accomplish the calibration and determination of the incident spectrum, the experimental arrangement shown in Figure 1 was used. The bremsstrahlung radiation produced by the betatron was collimated and directed against a collimated 5" x 4" NaI detector. The beam was attenuated with various thicknesses of Aluminum to eliminate the large amount of low energy pulses incident on the detector. The hardening of the incident spectrum helps eliminate

pulse pile up and makes the determination of the maximum or end point energy much easier to discern. The intensity of the beam was monitored with a high pressure ionization chamber connected to a vibrating reed electrometer and chart recorder. The output of the detector was pumped by a pre-amplifier to a multichannel analyzer which was gated on with the electron injection pulse of the betatron. The gate delay and width was set to enclose the width of the bremsstrahlung pulse, so that the multichannel analyzer counted only during the time that bremsstrahlung was produced. This significantly reduced the background during the measurement. In addition, the pre-amplifier output was sent to an oscilloscope triggered by the betatron injection pulse. The time interval between injection and the bremsstrahlung pulse is related to the bremsstrahlung end point energy (the end point energy is proportional to the sine of the time interval between injection and the production of bremsstrahlung.[1]) Thus, a plot of the end point energy vs. time interval yields a calibration curve for the betatron.

The measured pulse height output was converted to an incident photon spectrum by an unfolding program which had been previously developed,[1] and had proven to be quite successful for unfolding high energy gamma pulse height spectra. The program had been improved for this work, in that separate channels were combined to form energy bins in accordance with the detector resolution, rather than with the ad-hoc technique of adding 10 channels at a time which had been done previously.

A typical result of this phase of the investigation is shown in Figure 2. There are several important points to note in this figure. To begin with, the sharp cut-off at the end point energy as indicated in the figure (at 8.1 MeV) allows for accurate calibration. This sharp

cut-off is a result of the finite bremsstrahlung cross section at the maximum energy (or the energy of the electron which produced the spectrum.) Secondly, since the experiment utilized "good geometry", it was anticipated that the incident spectrum would be the bremsstrahlung spectrum attenuated by the Aluminum. The theoretical bremsstrahlung spectrum was taken from Schiff,[2] while the attenuation coefficients were taken from the work of Grodstein.[3] It can be seen that good agreement is obtained with the experimental data when the incident spectrum is taken as an attenuated Schiff spectrum. This work with the NaI detector thus established the betatron energy calibration and the betatron spectrum.

III. Experimental Set-up for Determining Response of NE-213 Detector.

The experimental arrangement shown in Figure 3 was used to determine the pulse height response of the NE-213 detector. The bremsstrahlung beam was directed against the detector, and the pulse height output from the linear output of the photomultiplier was pumped by a pre-amplifier to an amplifier and then to the MCA. An additional amplifier was necessary for this phase of the experimental work because of the low output pulses produced by the detector. The voltage on the detector was maintained at 1500 V., since higher voltages saturated the pulses. The measurement of the beam intensity and the gating of the MCA was the same as used for the incident spectrum measurement. The betatron energy was monitored with the NaI detector located outside of the beam; its output was sent to an oscilloscope triggered by the betatron electron gun injection pulse. The time span between the electron injection and the bremsstrahlung pulse was read on the oscilloscope to ascertain the end point energy from the previously determined calibration curve.

IV. Experimental Results

The calibration of the NE-213-MCA combination was done with the radioactive sources ^{137}Cs, ^{60}Co and ^{22}Na. A typical (ungated) spectrum for ^{137}Cs is shown in Figure 4, which has the expected shape with a peak at the Compton edge. The calibration curve obtained with these sources is shown in Figure 5, where the Compton edge energy is plotted against channel number. Good linearity was achieved, and the combination of spectral shape and linearity indicated proper operation of the electronics. A typical result obtained from a bremsstrahlung spectrum is shown in Figure 6, where the recorded counts vs Energy are plotted. The curve shown is for an incident bremsstrallung end point energy of 5.0 MeV, which has a Compton edge at 4.76 MeV. Curves similar to Figure 4 were obtained for end point energies from 2 MeV to 9 MeV. Lower energies will be obtained with radioactive sources.

V. Remaining Work

The primary work which remains to be accomplished is to unfold the response function from the known incident spectra and the measured pulse height spectra, and to check the response against known sources. Some additional experimental checks will undoubtedly have to be made to accomplish this. It is anticipated that most of the remaining work will be completed this summer.

References

1. A. Shapiro and W. F. Stubbins, "Calibration of U.C. Betatron", Nuclear Engineering Report, University of Cincinnati, 1968.

2. L. I. Schiff, "Energy - Angle Distribution of Thin Target Bremsstrahlung", Physical Review, Vol. 83, No. 2, 252, July 1951.

3. Gladys White Grodstein, "X-Ray Attenuation Coefficients from 10 KeV to 100 MeV", NBS Circular 583, April, 1957.

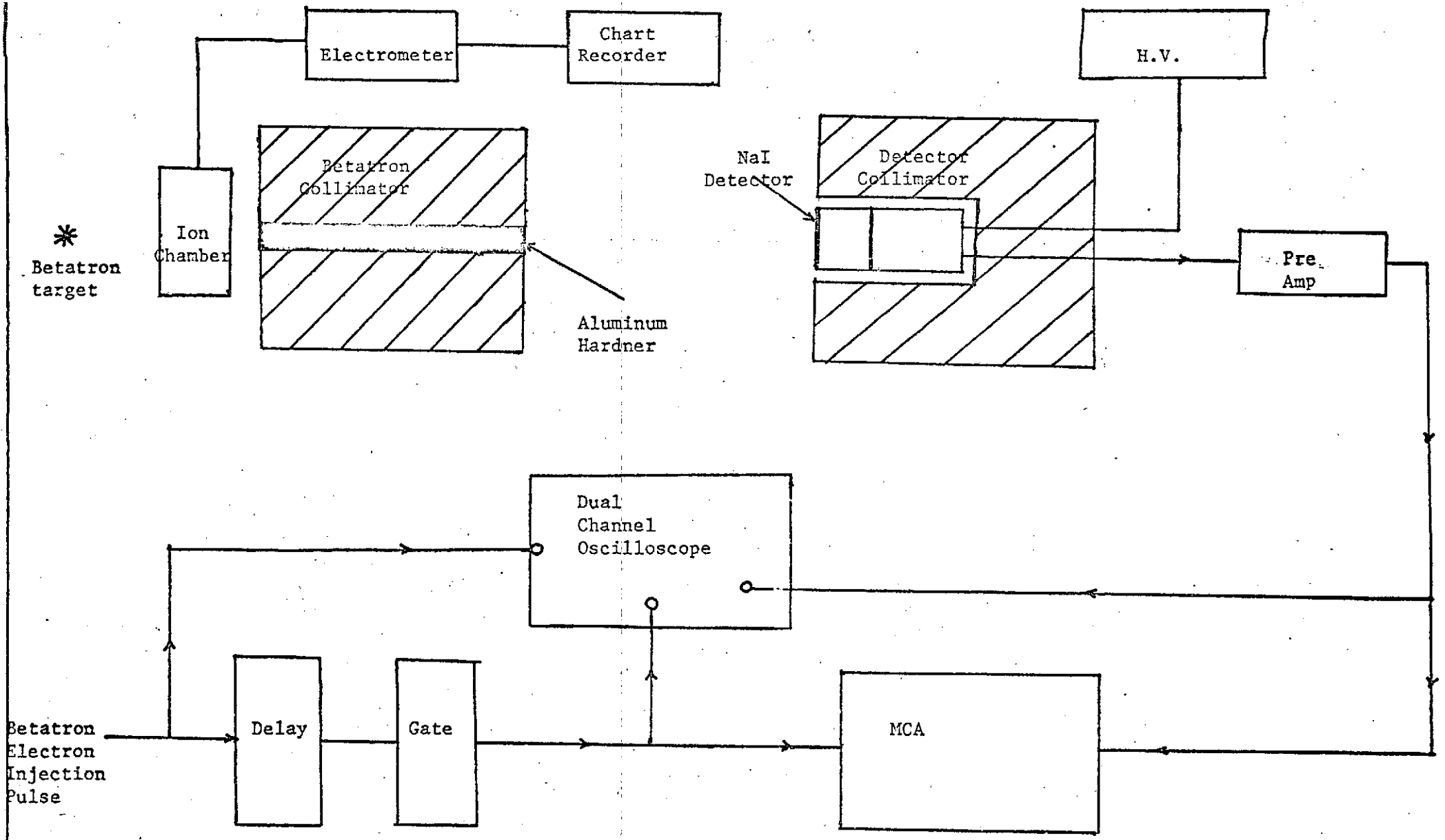

Figure 1

Experimental Set-up for Calibrating Betatron and Determining Incident Spectrum

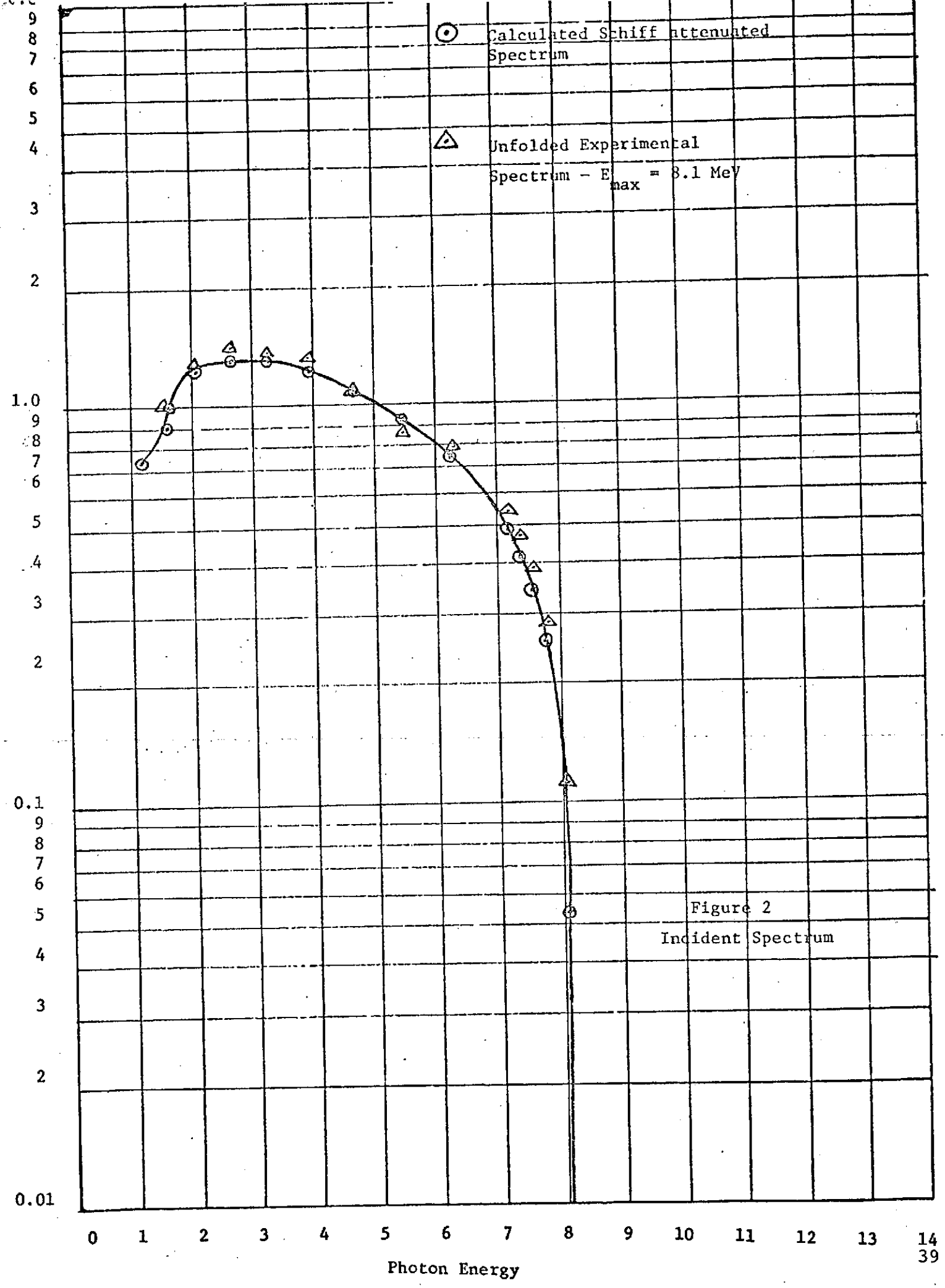

Figure 2

Incident Spectrum

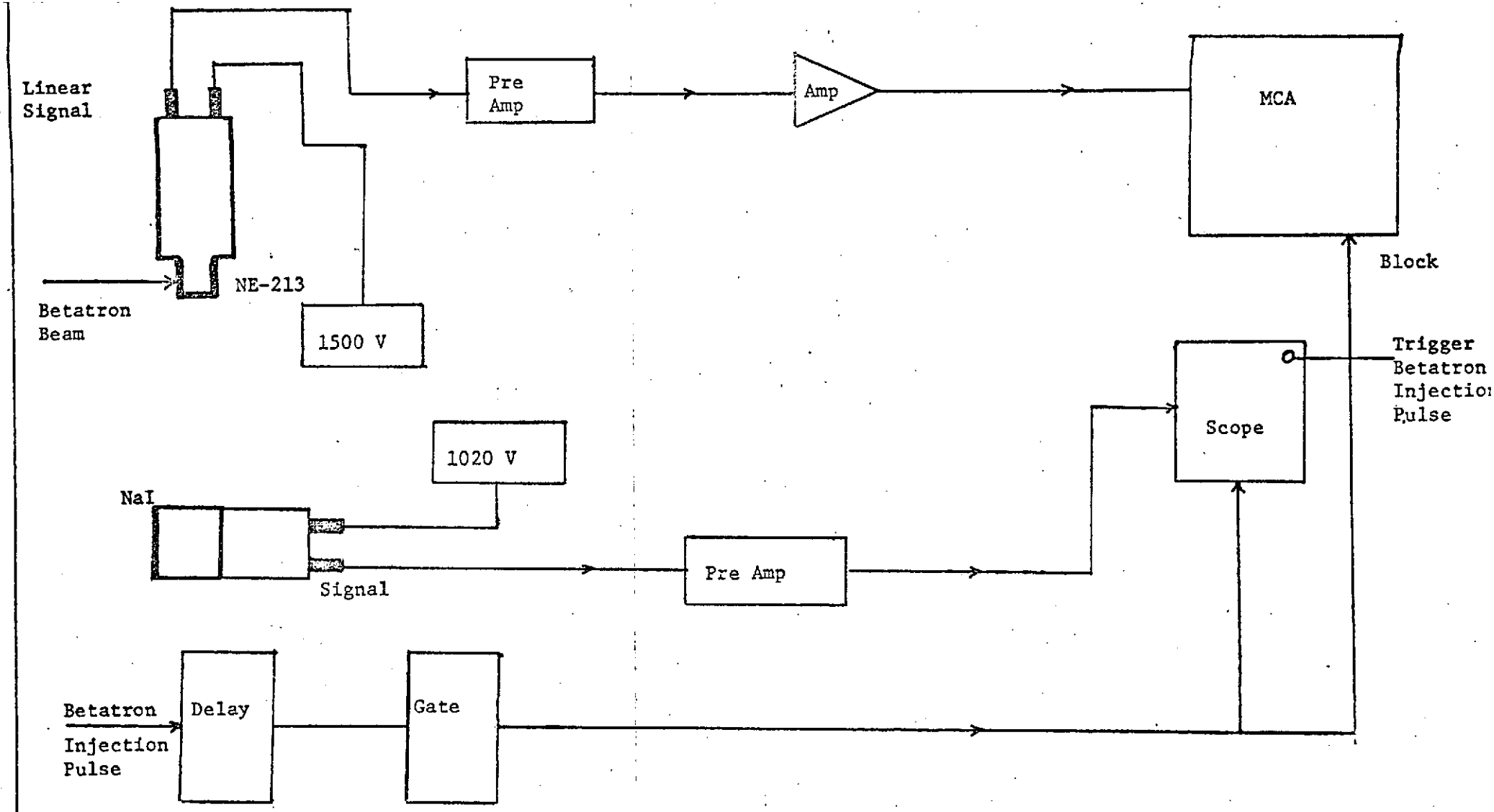

Figure 3

Experimental Set-up for Measuring Pulse Height Spectra of NE-213

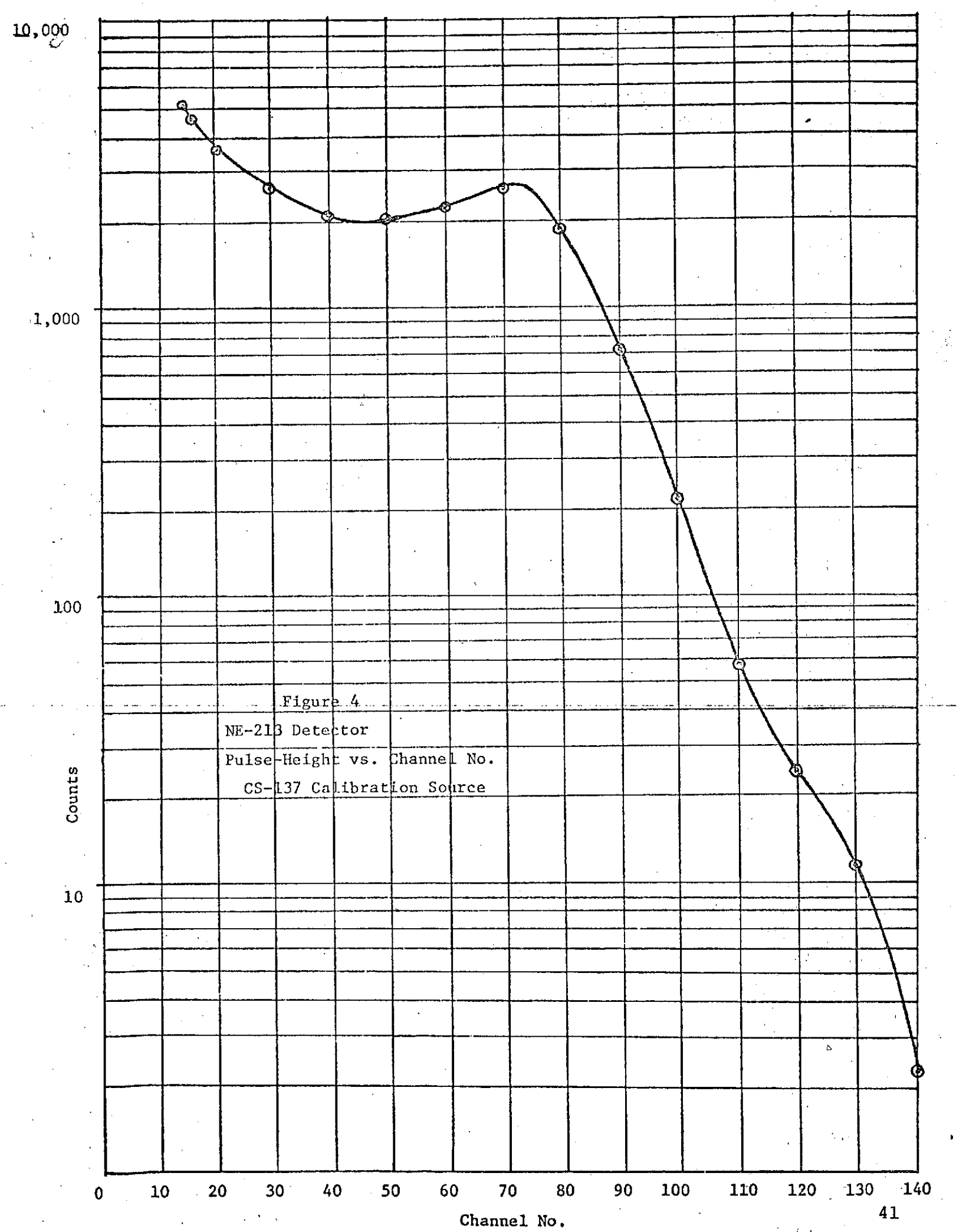

Figure 4

NE-213 Detector

Pulse-Height vs. Channel No.

CS-137 Calibration Source

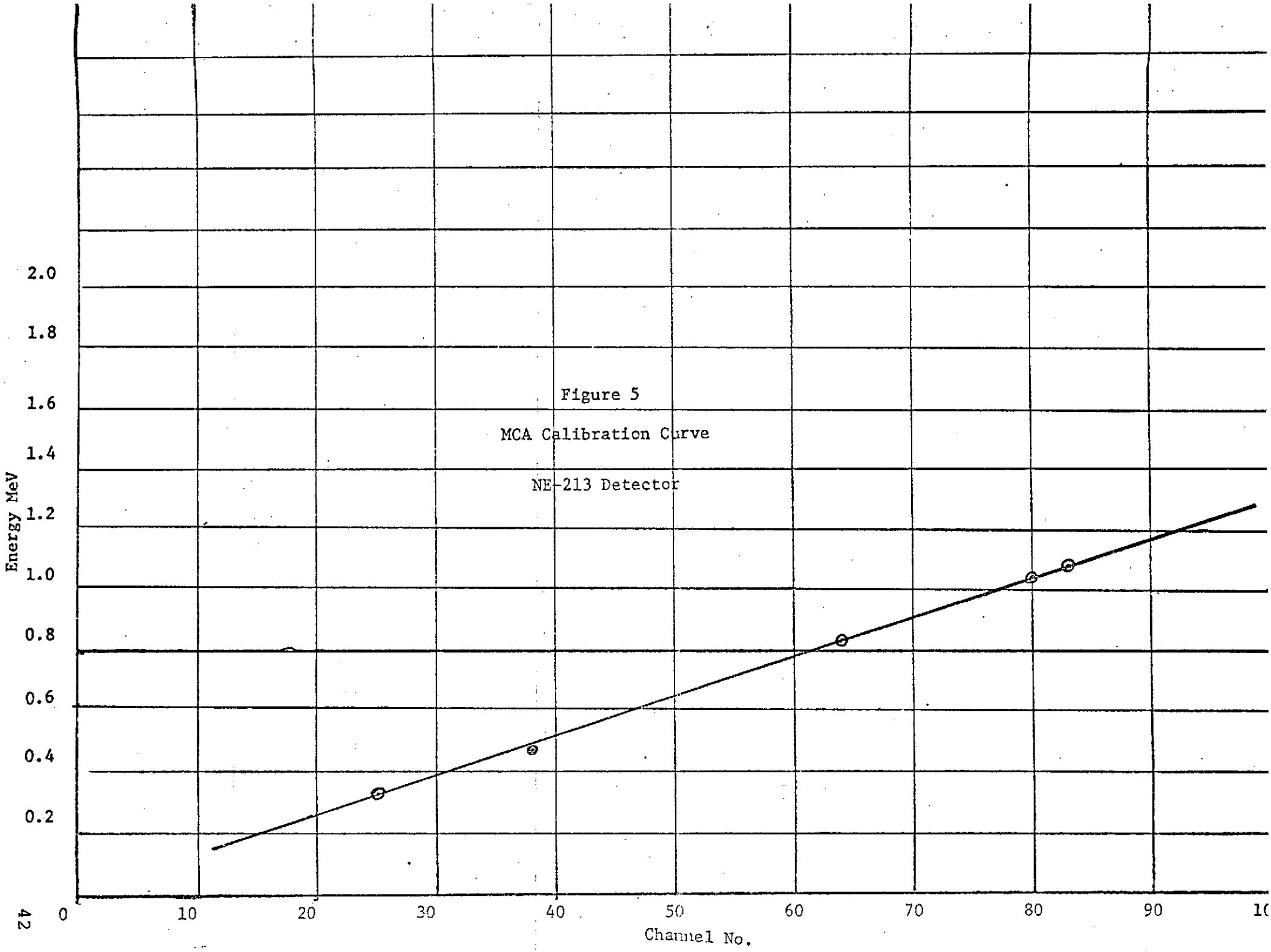

Figure 5

MCA Calibration Curve

NE-213 Detector